COMPOSITES UNITED

Strength capacity of bi-axially compressed UD strands at turning points of rotor blade loops and of hangers of network arch bridges.

Festigkeit bi-axial gedrückter UD-Stränge an Umlenkstellen von Rotorblattschlaufen und Hängern von Netzwerkbrücken.

- Derived on basis of Material Symmetry Facts and Cuntze's Failure Mode Concept FMC –

For aircraft engineering and for civil engineering

- Introduction with some Examples (intentionally from building industry)
- Design Idea of the UD Tape Strand Hangers
- Cuntze's Failure-Mode-Concept, Application to UD materials
- Design Verification focussing its Notions: Reserve Factor *RF*, *Eff (Werkstoffanstrengung)*, Failure Index $|F|$
- Discussion of Multi-axial Compressive Stress States in the Loops, *Eff* ↔ Strength Capacity
- Conclusions
- *Novel UD-model to Map the Influence of Porosity in the associated σ_2-σ_3-plane (formula, figure)*

Numerical details of many slides serve the later reader for understanding but will be not presented!

Non-funded investigation.

Prof. Dr.-Ing. habil. Ralf Cuntze VDI, engineer and hobby material modeler
Markt Indersdorf, Ralf_Cuntze@t-online.de, 0049 8136 7754

Fiber-reinforcing Products used in Engineering

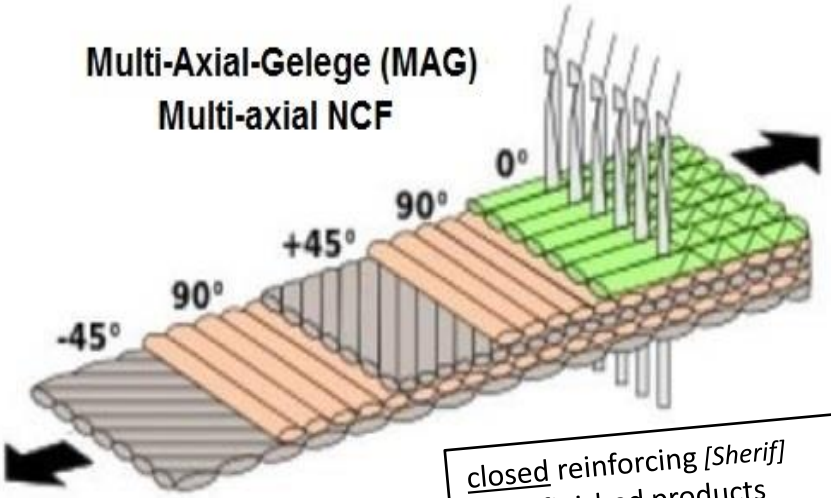

closed reinforcing *[Sherif]*
semi-finished products

pultrusion

Stab-Gitter
bar-grid

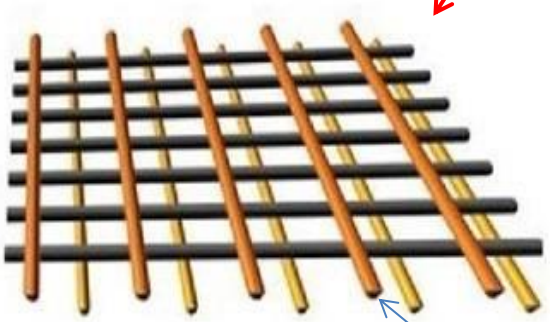

strands
heavy tow

textile

fiber grid mats

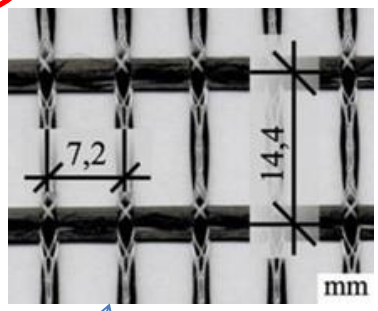

stiff when placing,
plate armouring

Q-mat and R-mat
deliverable

concrete matrix

polymer matrix

UD-Gelege
Non-Crimp Fabrics (NCF)

Gewebe
woven fabrics
Warp= Kette, Fill (Weft) = Schuss

open reinforcing *[Sherif]*
semi-finished products

pre-preg roll

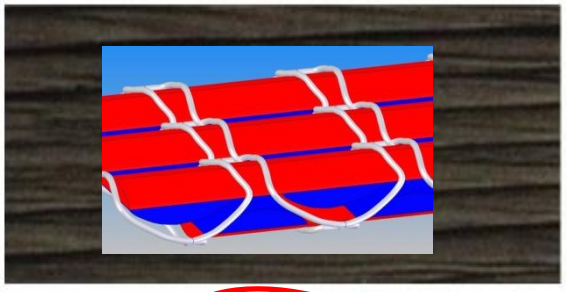

flexible when placing,
beam reinforcement

shotcrete

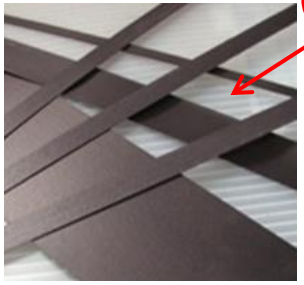

Tape, UD-lamina, Lamella

not in construction, polymer matrix

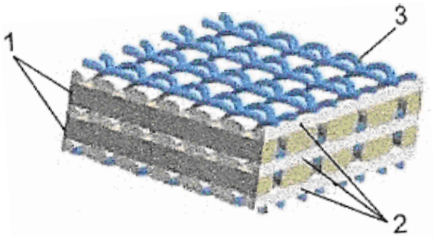

Lamelle ≡ *Gelege-Streifen,*
schmaler Gelege-Streifen ≡ strip, tape
breites Gelege-Stück ≡ sheet
Gelege = extremes Gitter, kein Faserabstand)

(a lamella may consist of one UD-layer or from an angle-ply layer in case of shear reinforcement)

Various Rotor Blades

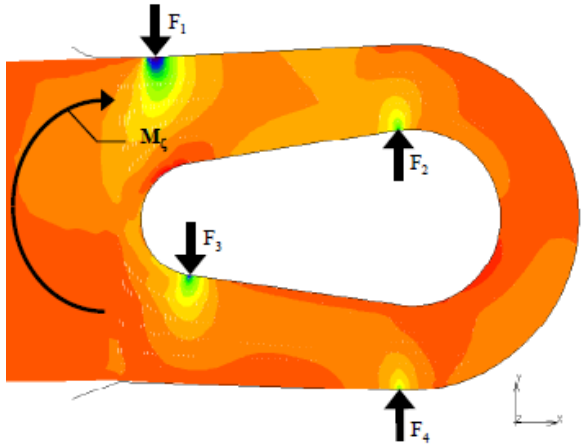

Courtesy: Eurocopter, Hauptrotorblätter

Rupert Pfaller

SAB 105mm CFK Heckrotorblätter

CFK-Zugglieder aus Strangschlaufen

seit 2003
CFK-
Strangschlaufen
für Krane und
Baumaschinen

EMPA, Prof. Urs Meier

Special Automated Fabrication Process (turning points dificulty)

Roving-
Placing Machine

Special automated additive manufacturing process with endless fiber strands stored on the fixed 'truss' nodes. Lightweight 'fiber pavilion' made of 60 CFRP/GRP components

*[**Knippers, Koslowski, ITKE Stuttgart; Menges, CD**]*

BUGA-Heilbronn

Art-work and Load-carrying structure

(Kunstwerk und Tragwerk)

Montage des 1,4 t leichten CFK-Brückensegments von BaltiCo (*© BaltiCo*)

Dr. Dirk Büchler

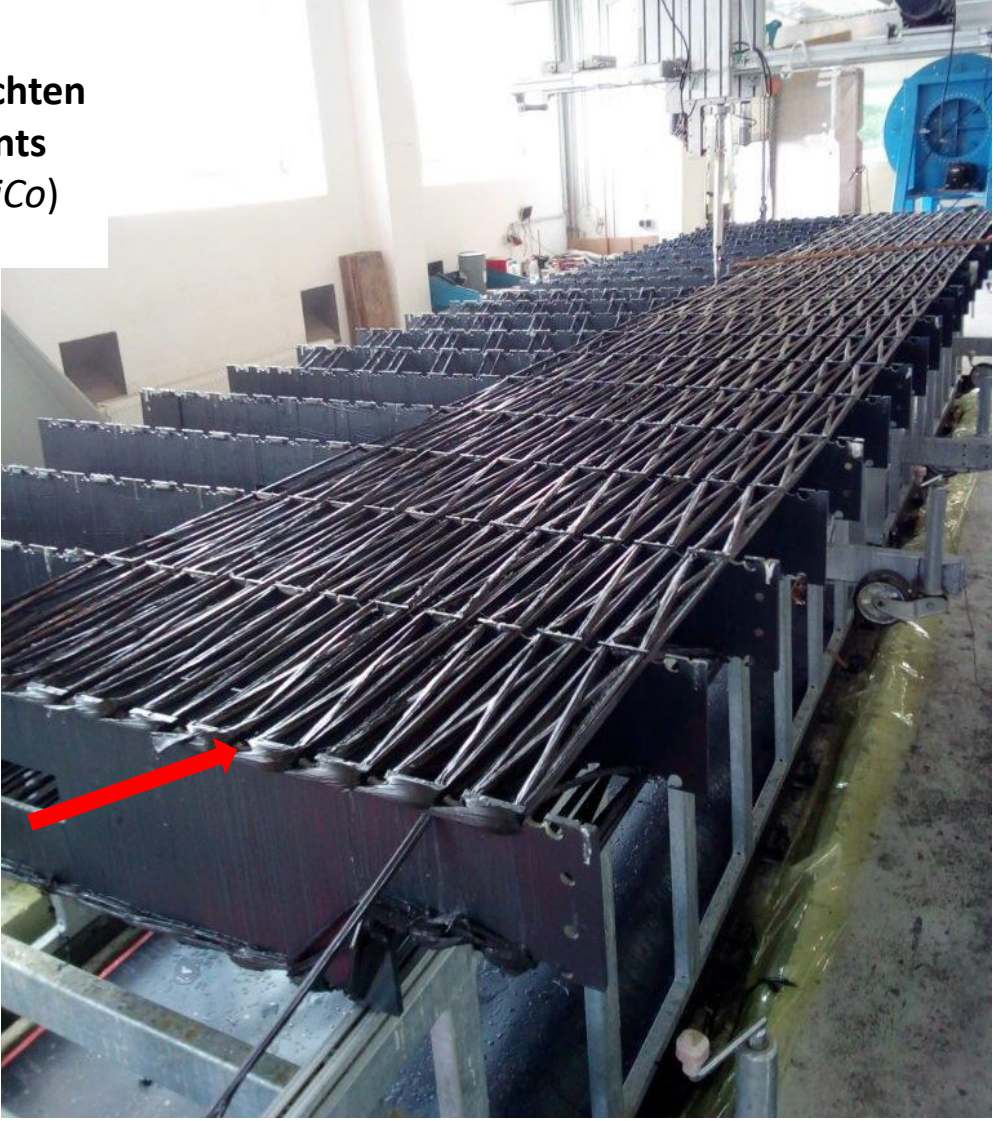

Sassnitz auf Rügen besitzt nun eine 25 m lange Brücke, hergestellt mittels CFK-Strang-Ablegetechnologie der BaltiCo GmbH.

Im Juli 2020 wurde eine Fahrrad- und Fußgängerbrücke aus kohlenstofffaserverstärktem Kunststoff (CFK) der Firma BaltiCo in Sassnitz montiert, was aufgrund der gerade einmal 1,4 Tonnen Gewicht eines einzelnen Segments leichter als üblich gelang und innerhalb eines einzigen Tages erfolgte.

Technische Potentiale

- Materialeinsatz senken
- Carbon Footprint senken
- Nachhaltiger Bauen
- Filigraner Bauen
- Neue Designfreiheiten nutzen
- Lebensdauer erhöhen
- Funktionen integrieren
- Kosten reduzieren

Dr. Dirk Büchler, BaltiCo,
CU Bau Vorstandsmitglied

menschliches Haar
und Carbonfaser

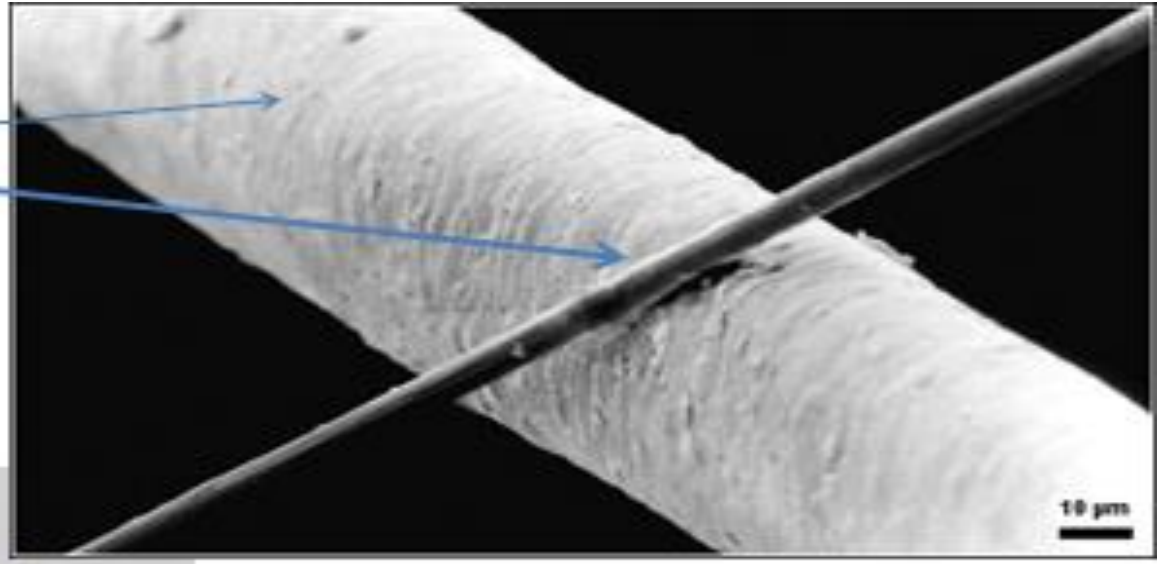

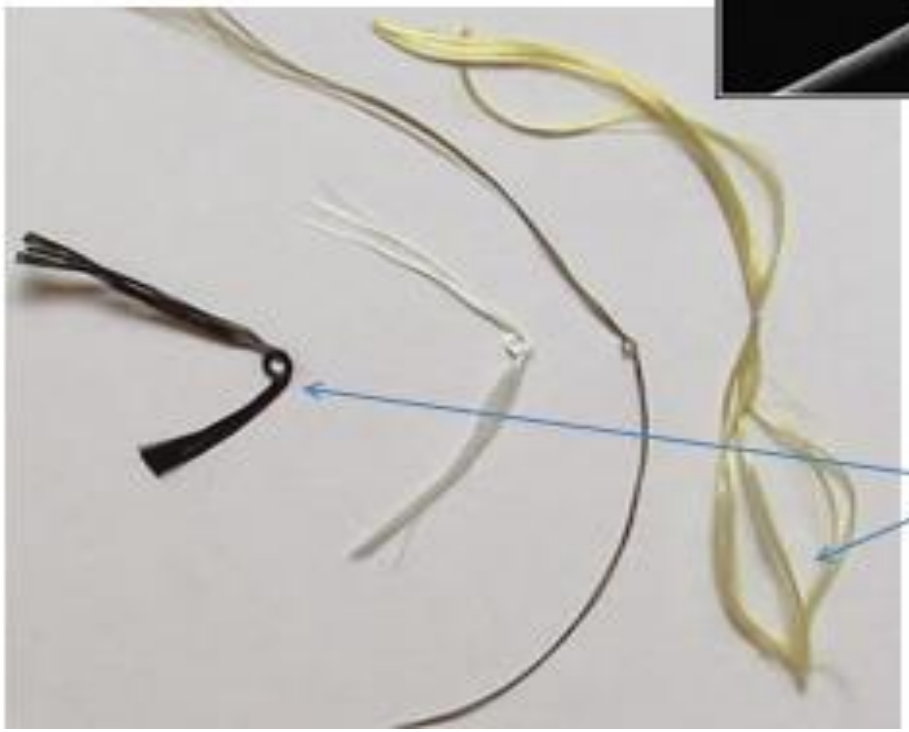

Fasern:
Carbon, Glas, Basalt,
Aramid

PROBLEMS:

(left, down) knot-test to visualize brittleness grade and fiber bending radius limits of fibers, (right) a comparison of a carbon-fiber (Ø 7 µm) versus a hair (necessary for radius of armoring cages

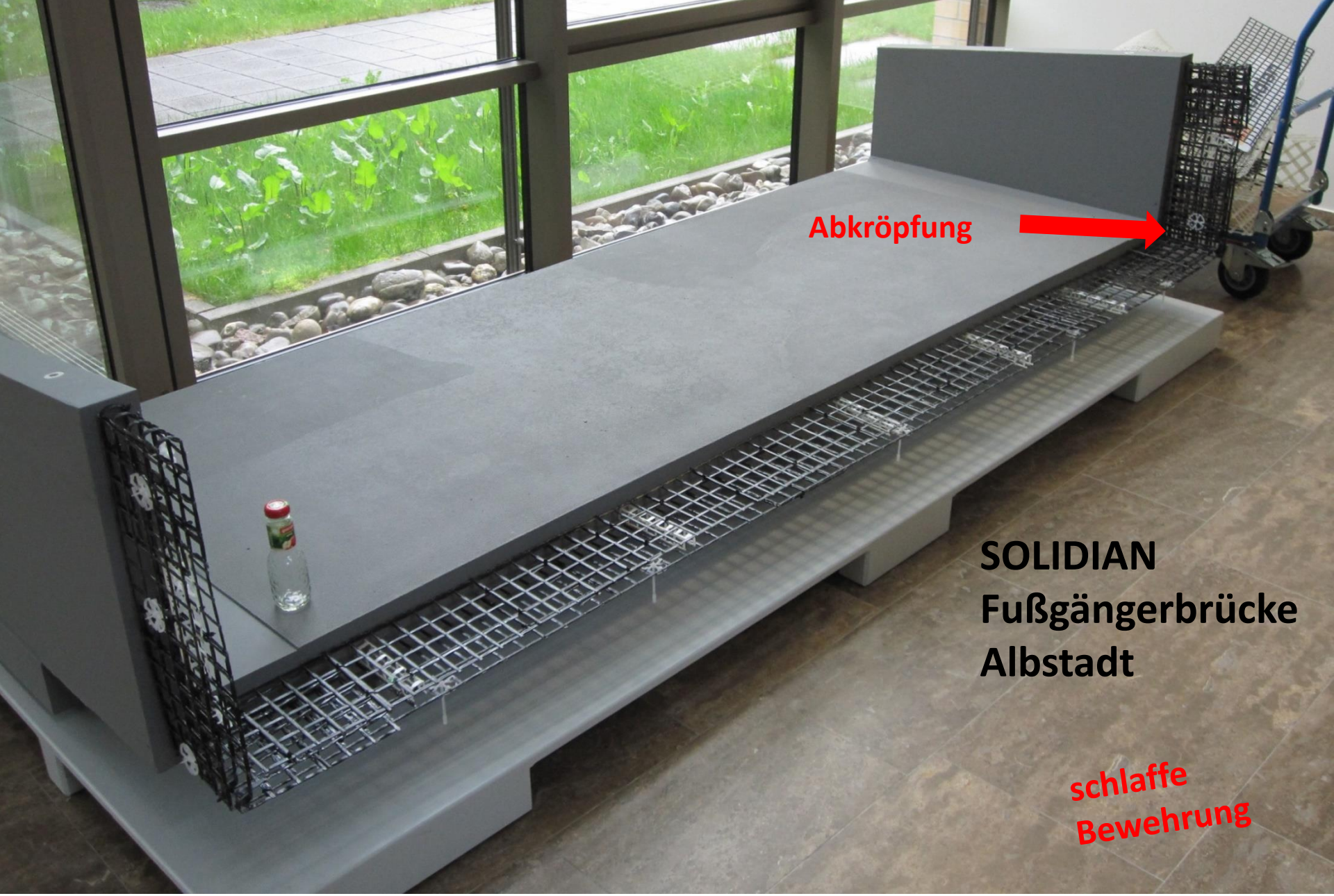

Wäre zu dimensionieren nach: D96 DAfStb UA Nichtmetallische $_{nm}$ Bewehrung:
DAfStb-Richtlinie "Betonbauteile mit nichtmetallischer Bewehrung"

CFK-Hänger der Stuttgarter Stadtbahn-Brücke

The Stuttgart Stadtbahn bridge, installed over the A8 motorway in May 2020 in Germany, is the world's first network arch bridge that hangs entirely on tension elements made of carbon fiber-reinforced plastic (CFRP).
The 72 hangers are produced with Teijin (Wuppertal, Germany) carbon fiber, Tenax, by Carbo-Link AG (Fehraltorf, Switzerland).

[Dr. Winistörfer, Carbo-Link,
Prof. Urs Meier, EMPA]

Design challenge: Fiber Stress Concentration around the Loop

1. High secondary stresses (stress concentrations) occur around the bolt area when loading laminated strand loops. The more rigid the fibre and the "thicker" the loop is, the higher the secondary stresses are that will be generated.

Non-laminated strand loops solve this problem. Such a strand loop is made of a very thin UD tape of only 0.12 mm thickness. This tape is continuously laid in the desired number of layers around corresponding deflection bodies (bolts, pins) by an 'endless tape lay-up device'.. There is no full bond between the individual layers, just friction bond. The last layer is laminated with the penultimate layer on a length of about 10 cm and anchored with it. *[Winistörfer, A.; Mottram, T.: Finite Element Analysis of Non-Laminated Composite Pin-Loaded Straps for Civil Engineering, Journal of Composite Materials, Vol. 35, 2001. Carbo-Link and EMPA Dübendorf, Prof. Urs Meier*].

When loading the '**friction bond**' tape strand loop, a relatively even stress distribution is achieved due to relative shifts possible between the adjacent tape layers. The load transmission between the layers is carried out by friction. Better exploitation of the fiber strength over thickness!

2. Lateral supports increase the load-bearing capacity of strand loops made of carbon fibre. This indicates that in dimensioning of loops it is necessary to apply a 3D-strength analysis (VDI 2014 Part 3, editor: R. Cuntze).

3. Full bond solutions suffer from tribologic wear ('fretting') over operational time which impacts the fatigue life. Protection is to foresee (Teflon, not topic here).

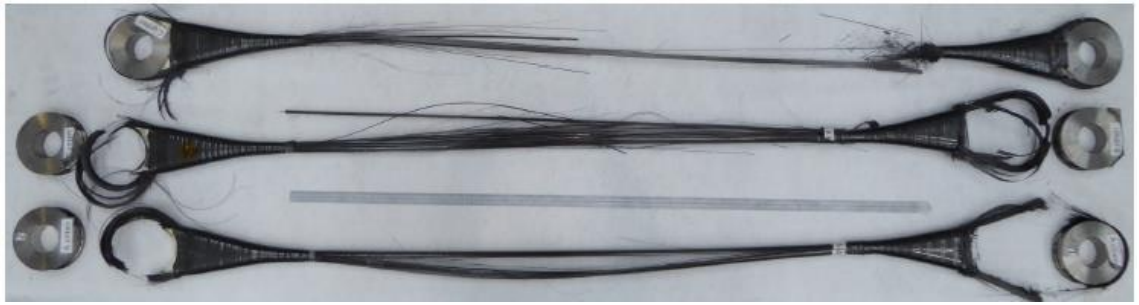

Production experience: **full bond**
When putting layer upon layer the 'winding tension force' will compress the former layer and reduce the efficiency of the former layer. This situation is improved by an optimal choice of the 'winding tension force' in the process together with intermediate consolidation.

full bond, laminated

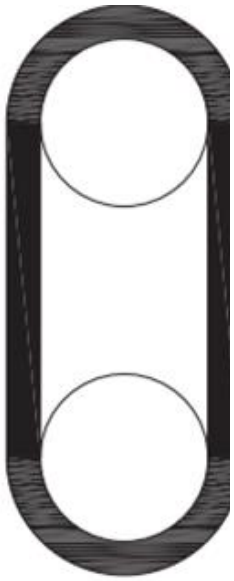

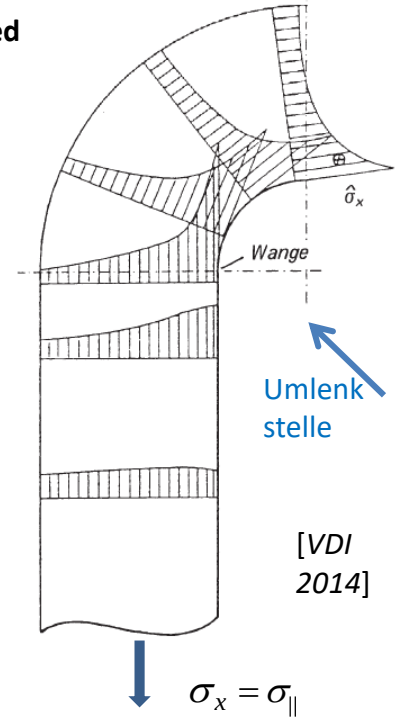

[*VDI 2014*]

$\sigma_x = \sigma_{||}$

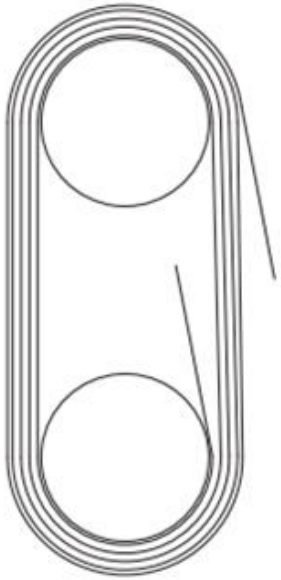

friction bond, not commonly cured biegeschlaffe Konstruktion der Strangschlaufe [*Carbo-Link*]

Fabrication of CFRP-Hangers *(pin-loaded tendons):* Tensile rods with Tape Loop ends

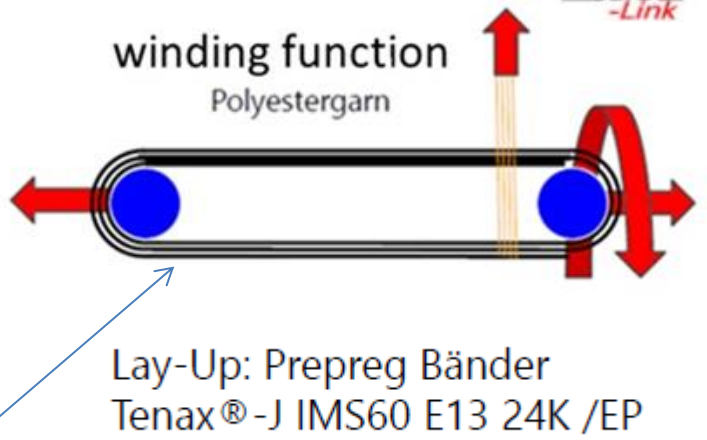

- **Built up by a narrow ‘endless tape lay-up device’.**
- **Round tensile rod region is generated by wrapping a polyester yarn around.**
- **Dyneema sliding layer between thimble and pin.**
- **UD-strand is constrained in lateral direction in the thimble by the side supports.**

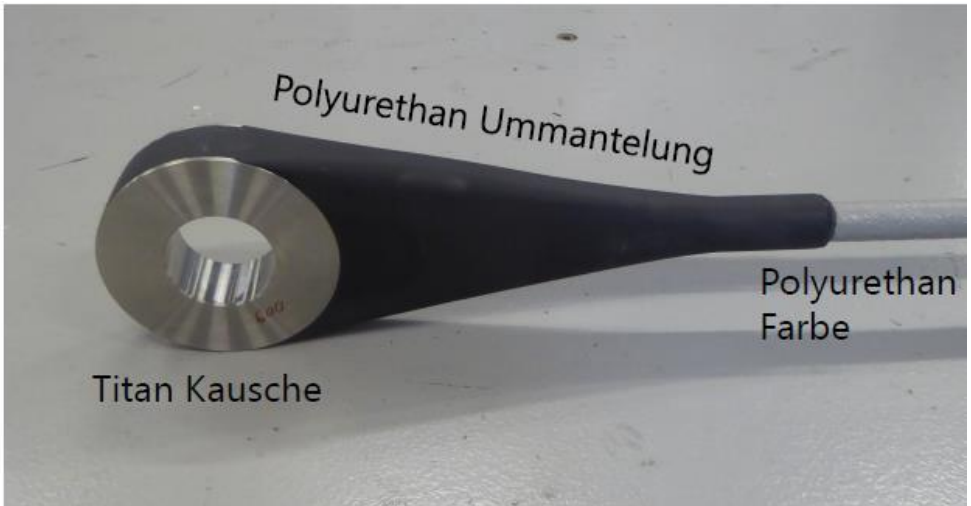

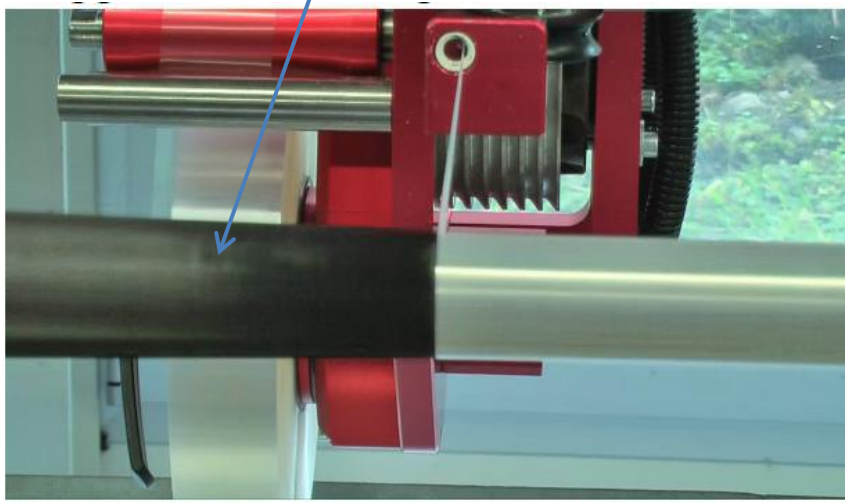

Bending of Filaments and of UD Strands and Tape Loops

friction-bond tape laying

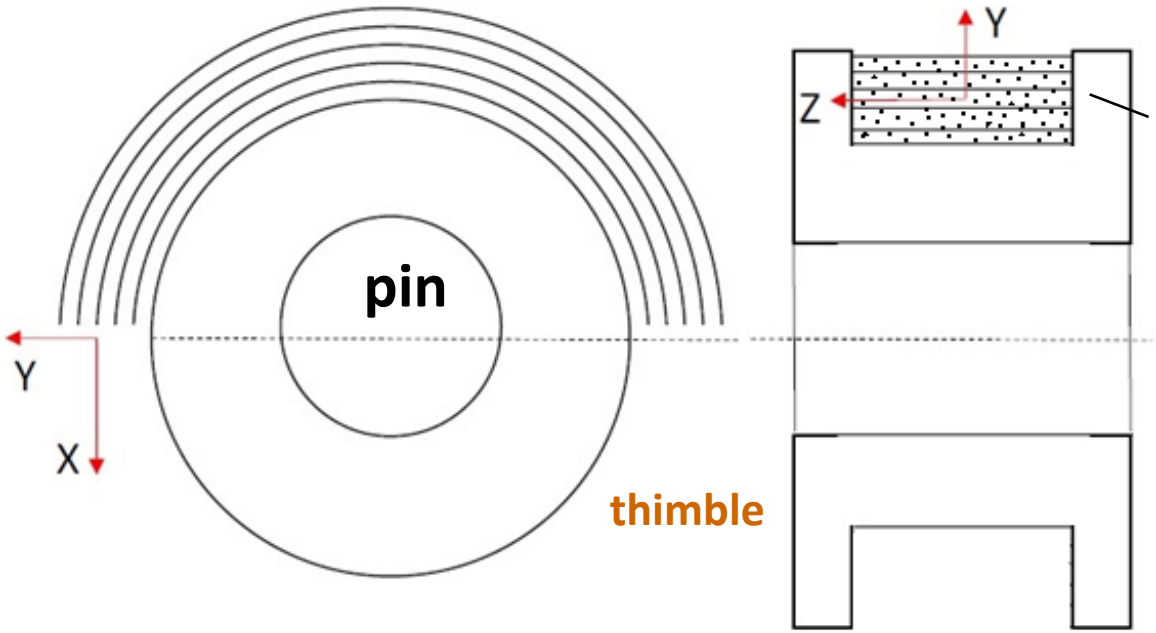

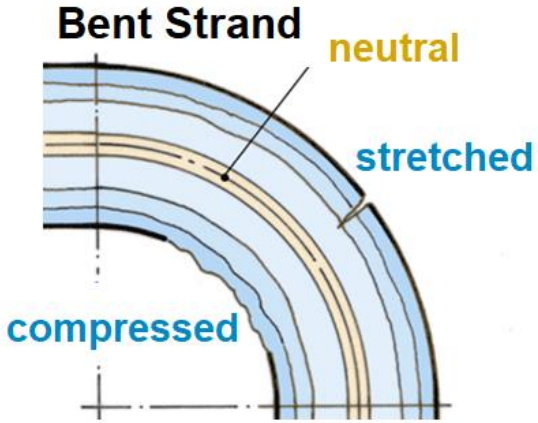

bent pre-preg tape.

(2)Crooked fibers do not carry load !

The turning locations are the challenging sites →

Structural Modelling, geometry, loading *[propriety sbp consultants, Stuttgart]*

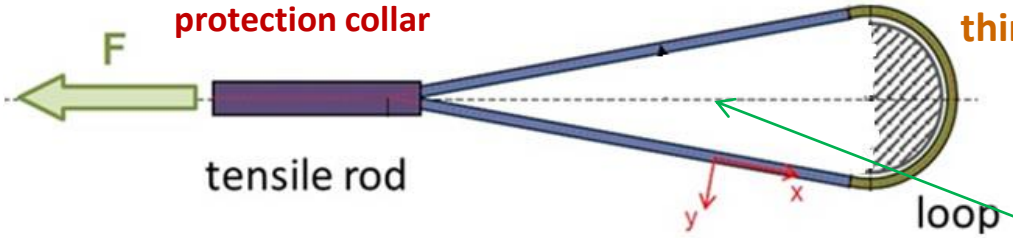

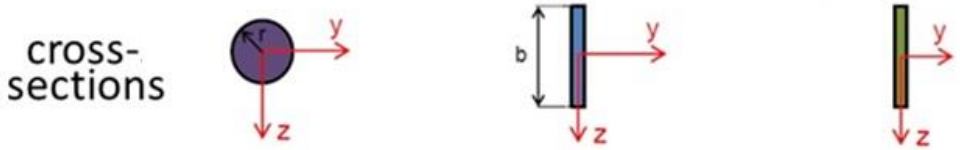

TiAl6V4
structural steel
PVC foam insert
CFRP (UTS 50)
pre-preg tape

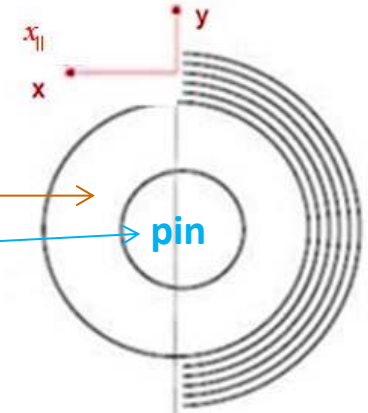

stress situation of the thimble

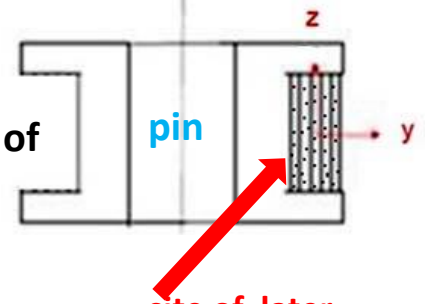

site of later 3D verification

$\sigma_2^c \leftarrow \sigma_z^c, \quad \sigma_2^c \leftarrow \sigma_y^c$

Dimensioning Load Cases:

Axial loading, Pin rotation, Hygro-thermal effect, Friction.

The stresses in a loop can be roughly calculated if they are taken as the same as those in a thick-walled tube. This will also make it immediately clear that, in addition to the tangential stresses, radial stresses also dominate, being at their maximum at the inner edge , precisely, where the tangential stresses are also the largest!

These can be easily calculated from the transferred force *F* and the geometrical data for

Tenax® CARBON FIBERS

Definition	Grade		Filament Count	Tensile Strength	Tensile Modulus	Tensile Elongation	Diameter	Density	Electrical Resistivity
				MPa	GPa	%	µm	g/cm³	ohm. cm
High Tensile	UTS50	12K	12000	4900	240	2	6.9	1.8	1.6×10^{-3}
		24K	24000	5000	240	2.1	6.9	1.79	1.8×10^{-3}

sbp: schlaich, bergermann & partner

3D-Design is mandatory and a Stress Assessment Tool

In the development of UD structural components
the application of 3D-validated Strength-Failure-Conditions SFCs ('criteria') $F = 1$
is one essential pre-condition for achieving in design verification
the required fidelity for structural product certification and production.

What is to provide?
3D-Strength Failure Conditions SFC to verify that Onset-of-Fracture does not occur.

That menas for the creation of the SFCs :
Using a **'Global'** Failure Function formulation **(Drucker-Prager, Tsai)** with $F = 1$ or
using a **'Modal'** Failure Function formulation **(Mises, Cuntze)** with
the so-called **Material Stressing Effort (Werkstoffanstrengung)** Eff **= 100%.**

Eff = 100% is better understood by the engineer
and is valid in non-linear analysis where
Eff remains 100% during degradation that follows 'Onset-of-Fracture' !

'Modal' versus **'Global'** SFCs:
Modal means that only a test data set of one failure mode domain is mapped whereas global (Drucker-Prager isotropic, Tsai UD) means that mapping is performed over several mode domains, shear fracture mode SF with normal fracture mode NF.
The bottle-neck of global SFCs respectively 'Single Failure Surface Descriptions ' is, that any change in one of the 'forcibly married' modes requires a new global mapping which changes the failure curve in the physically not met mode, too.
Modal SFCs like Mises an Cuntze's SFCs generate real equivalent stresses (see Annex)

Experience with Material-Symmetry → *a physically sound Basis for the Generation of SFCs*

1 If a material element can be homogenized to an ideal crystal (= frictionless),

then material symmetry demands for the Isotropic Material are:

- 2 *elastic 'constants', 2 strengths, 2 fracture toughness values, 2 'basic' invariants* I_1, J_2 and *2 strength failure modes*, for *yielding* two (NY, SY) and for *fracture* two (NF, SF) (→ for isotropic materials may be recognized a 'generic number' of 2. One needs just 2 invariants for formulate SFCs. This is valid as long as a one-fold acting failure mode is to describe by the distinct SFC and not a multi-fold one, such as for $\sigma^t_{II} = \sigma^t_{III}$, $\sigma^c_{II} = \sigma^c_{III}$)
- 1 *so-called physical parameter (such as the coefficient of thermal expansion CTE, and the coefficient of moisture expansion CME, friction μ , etc.)*

and for Transversely-isotropic UD-material :

- a generic number of 5 is witnessed for strengths etc and 2 for physical parameters.

2. *A real solid material model is represented by a description of the ideal crystal (frictionless) + a description of its friction behavior.* → Mohr-Coulomb requires for the real crystal another *physical parameter the inherent material friction value μ, namely is* 1 *for isotropic materials and* 2 *for UD materials*

3 Fracture morphology gives finally evidence

Each strength corresponds to a distinct *strength failure mode* and

to a distinct *strength fracture type*, to Normal Fracture (NF) or Shear Fracture (SF).

author → **Material Symmetry-dedicated Derivation of FMC-based 'Modal' SFCs** →

UD-SFCs for 'Onset of fracture failure', mode interaction, and value domains

FF1 $Eff^{\parallel\sigma} = \breve{\sigma}_1 / \bar{R}^t_{\parallel} = \sigma^{\parallel\sigma}_{eq} / \bar{R}^t_{\parallel}$, $\breve{\sigma}_1^{\,*} \cong \varepsilon^t_1 \cdot E_{\parallel}$ filament strains from FEA

FF2 $Eff^{\parallel\tau} = -\breve{\sigma}_1 / \bar{R}^c_{\parallel} = +\sigma^{\parallel\tau}_{eq} / \bar{R}^c_{\parallel}$, $\breve{\sigma}_1 \cong \varepsilon^c_1 \cdot E_{\parallel}$ 2 filament modes

IFF1 $Eff^{\perp\sigma} = [(\sigma_2+\sigma_3) + \sqrt{(\sigma_2-\sigma_3)^2 + 4\tau_{23}^2}\,]/2\bar{R}^t_{\perp} = \sigma^{\perp\sigma}_{eq} / \bar{R}^t_{\perp}$ Puck's mode A

IFF2 $Eff^{\perp\tau} = [(\frac{\mu_{\perp\perp}}{1-\mu_{\perp\perp}})\cdot(\sigma_2+\sigma_3) + \frac{1}{1-\mu_{\perp\perp}}\sqrt{(\sigma_2-\sigma_3)^2+4\tau_{23}^2}\,] / \bar{R}^c_{\perp} = +\sigma^{\perp\tau}_{eq} / \bar{R}^c_{\perp}$ 3 'matrix' modes

IFF3 $Eff^{\perp\parallel} = \{[2\mu_{\perp\parallel}\cdot I_{23-5} + (\sqrt{(2\mu_{\perp\parallel})^2 \cdot I_{23-5}^{\,2} + 4\cdot \bar{R}_{\perp\parallel}^{\,2}\cdot(\tau_{31}^2+\tau_{21}^2)^2}\,]/(2\cdot \bar{R}_{\perp\parallel}^{\,3})\}^{0.5} = \sigma^{\perp\parallel}_{eq} / \bar{R}_{\perp\parallel}$

$a_{\perp\perp}$

with $I_{23-5} = 2\sigma_2\cdot\tau_{21}^2 + 2\sigma_3\cdot\tau_{31}^2 + 4\tau_{23}\tau_{31}\tau_{21}$ [Cun04, Cun11]

Modes-Interaction $Eff^m = (Eff^{\parallel\tau})^m + (Eff^{\parallel\sigma})^m + (Eff^{\perp\sigma})^m + (Eff^{\perp\tau})^m + (Eff^{\perp\parallel})^m$

with influence IFF on FF: $= 1 = 100\%$ is 'onset of failure'

Reibung, μ !

with mode-interaction exponent $2.5 < m < 3$ from mapping test data

Typical friction value data range: $0.05 < \mu_{\perp\parallel} < 0.3$, $0.05 < \mu_{\perp\perp} < 0.2$

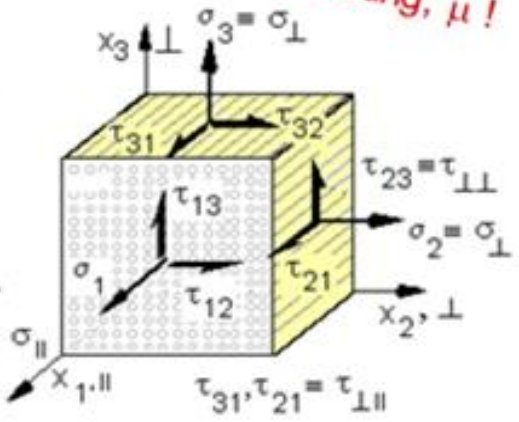

Eff:= material stressing effort (Werkstoffanstrengung), *R*:= UD strength, σ_{eq}:= equivalent stress.
Eff:= artificial word, fixed with QinetiQ in 2011, to have an equivalent English term.
Poisson effect considered*: bi-axial compression strains a filament without any σ_1
t:= tensile, c: = compression, ∥ : = parallel to fibre, ⊥ := transversal to fibre

With the SFCs above the author became winner of the World-Wide-Failure-Exercise-I and was top-placed in WWFE-II.
The derivation of the friction value from the original friction parameter $a_{\perp\perp}$ ($\mu_{\perp\perp}$) is presented on an attached slide.
The Effs are derived on basis of the 'Proportional Loading (stressing) Concept'.

‘Modal ‘ SFCs require the Interaction of the single Modes *

$$Eff = \sqrt[m]{(Eff^{\text{mode 1}})^m + (Eff^{\text{mode 2}})^m + ...} = 1 = 100\% , \quad if \quad \text{Onset-of-Failure}$$

Eff = 100% represents the mathematical description of the surface of the failure body

The interaction of adjacent failure modes is modelled with the ‘series failure system”.

That permits to formulate the total material stressing effort from all activated failure modes as ‘accumulation’ of *Eff*s or *in other words* as the sum of all the *failure danger proportions*.

m is mode interaction exponent.

Similarity of problem : ***commonly activated failure modes increase failure probability***

* In stability, the interaction of modes is ‘managed’ by design: *Placing all other modes far away of the global mode !*
* In strength, all is more coupled, however, *the size of the equivalent stress of a UD mode can be used as design driver*
* In bonding, separation of the design critical adhesive failure from cohesive substrate failure.

From mapping experience in the transition zone of modes:

The interaction exponent *m* for brittle materials ($R^c/R^t > \approx 3$) the value is about *m* = 2.6.

A smaller *m* is conservative, on the ‘safe side’.

2D-Interaction, demonstrated in the IFF cross section, CFRP failure curve

2D stress state within the lamina, m=2.7

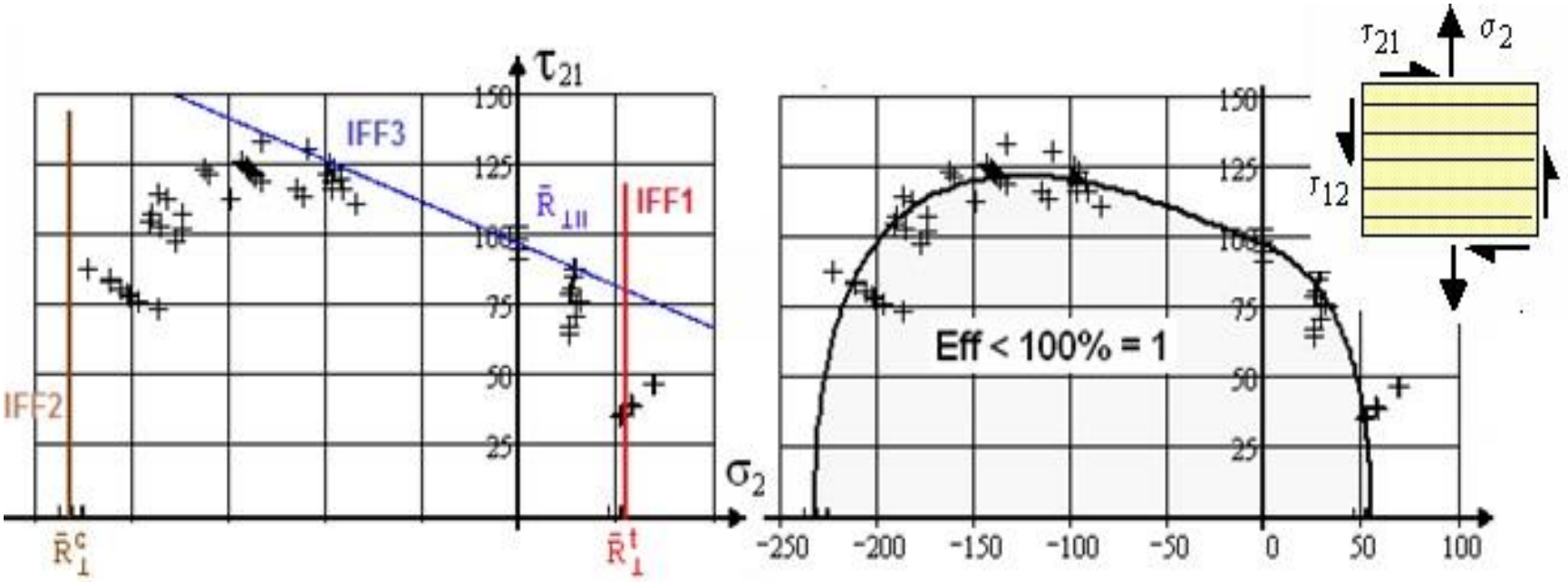

Fracture body of the UD material (lamina, lamella, sheet, tape) for 2D and 3D stress states

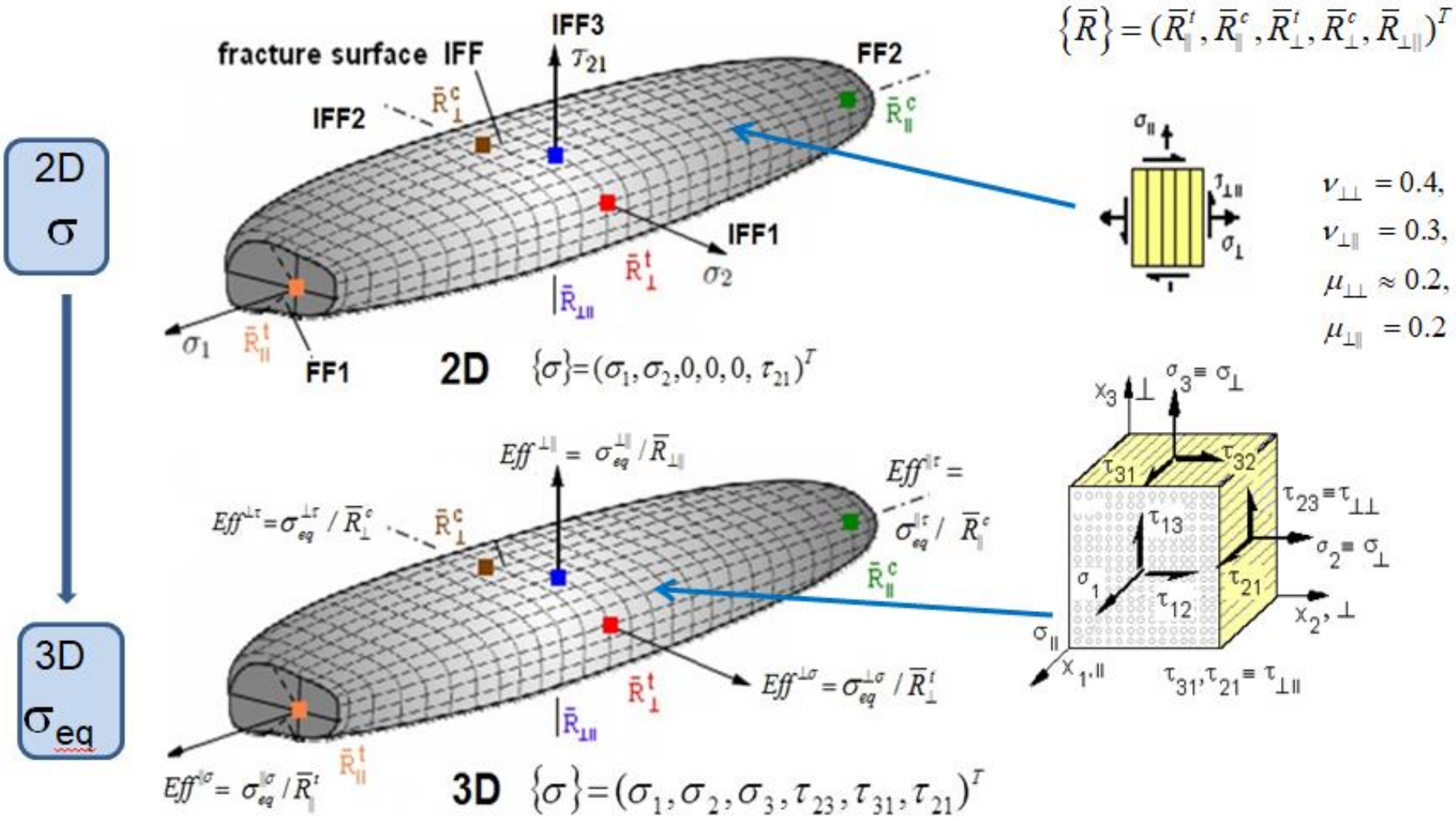

The use of the entity Eff excellently supports **'understanding the multi-axial strength capacity of materials'.**

Independently of the multi-axial stress state: Eff (Werkstoffanstrengung) can never exceed 100%!

The measured UD fracture stress curves in the quasi-isotropic σ_2-σ_3-plane. Scheme of the 90°-wound tension/compression-torsion test specimen

Quasi-isotropic plane, where the 3D-stress state in the **turning point** takes place.
Shear fracture domain, IFF2.

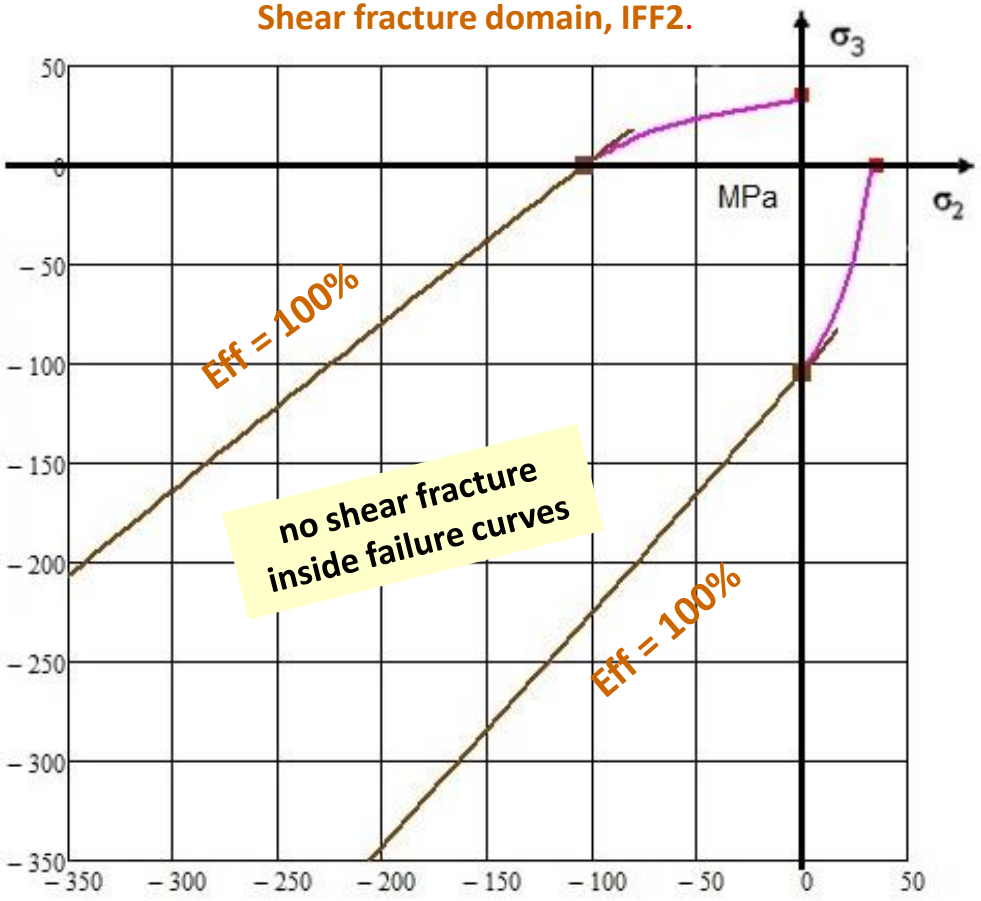

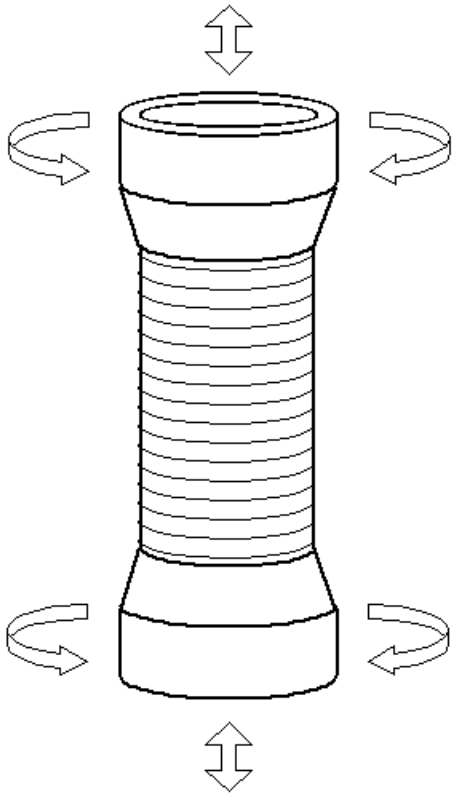

+ p_{hyd}-loading

Mind, however: Due to the Poisson effect, bi-axial compression leads to a tensile straining which usually is easily captured by an additional amount of tensile stress in the axially oriented fibers.

Demonstration of Static Strength in Design Dimensioning → Design Verification

The Design Strength of a structural part is demonstrated if

- no relevant strength failure (= limit state $\mathcal{G} = F - 1 = 0$ of a failure mode) is met
- all dimensioning load cases consider

  Each distinct load case with its various Failure Modes

  by a positive Margin of Safety $MoS > 0$ or a Reserve Factor $RF > 1$.

RF := 'Load View' of the Design Verifier

A further increase of the loading is allowed

if $RF > 1$ and similar if $Eff < 100\% = 1$.

Reserve Factor (is load-defined) : as ***RF = failure load / applied Design Load***

Non-linear analysis finishes if $Eff = 100\%$ which means $RF = 1$

$$RF = \frac{\text{(non-linearly) Predicted Failure Load}}{j \cdot \text{Design Limit Load}} > 1.$$

with $j :=$ design factor of safety, $DUL = j_{ult} \cdot$ Design Limit Load

Material Reserve Factor : ***f_{Res} = strength / applied stress ≡ Puck's Stretch Factor f_S***

$$f_{Res} = \frac{1}{Eff} = \frac{\text{Strength Design Allowable } R}{\text{Stress at } j \cdot \text{Design Limit Load}} > 1.$$

essential for linking →

if linear analysis: $f_{Res} = RF = 1 / Eff$, $Eff \equiv Puck's\ f_E$

'Proportional loading (stressing) concept'

f_{Res} in construction $= (R_k / \gamma_M) / (\sigma \cdot \gamma_S) = R_k \cdot \gamma_S / (\sigma \cdot \gamma_M)$

with γ_M, γ_S the partial safety factors applied for material and stress

Discussion of Lateral Stress States in General and in the UD-hanger Strand Loop. Visualisation of the *Eff* values of 3 different Compression Stress States. *IFF 2-mode domain*

IFF2 $$Eff^{\perp\tau} = [(\frac{\mu_{\perp\perp}}{1-\mu_{\perp\perp}})\cdot(\sigma_2+\sigma_3) + \frac{1}{1-\mu_{\perp\perp}}\sqrt{(\sigma_2-\sigma_3)^2+4\tau_{23}^2}] \;/\; \bar{R}_\perp^c = +\sigma_{eq}^{\perp\tau} / \bar{R}_\perp^c$$

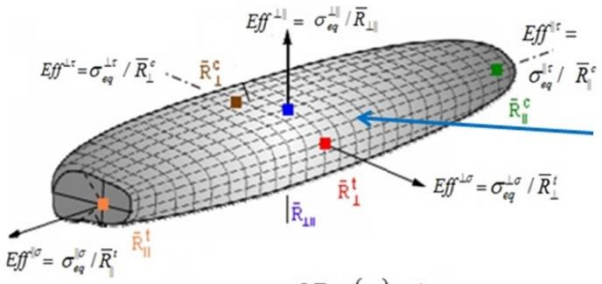

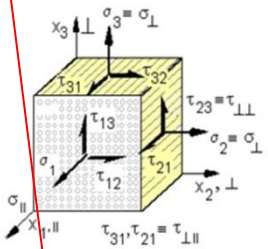

3D $\{\sigma\} = (\sigma_1, \sigma_2, \sigma_3, \tau_{23}, \tau_{31}, \tau_{21})^T$

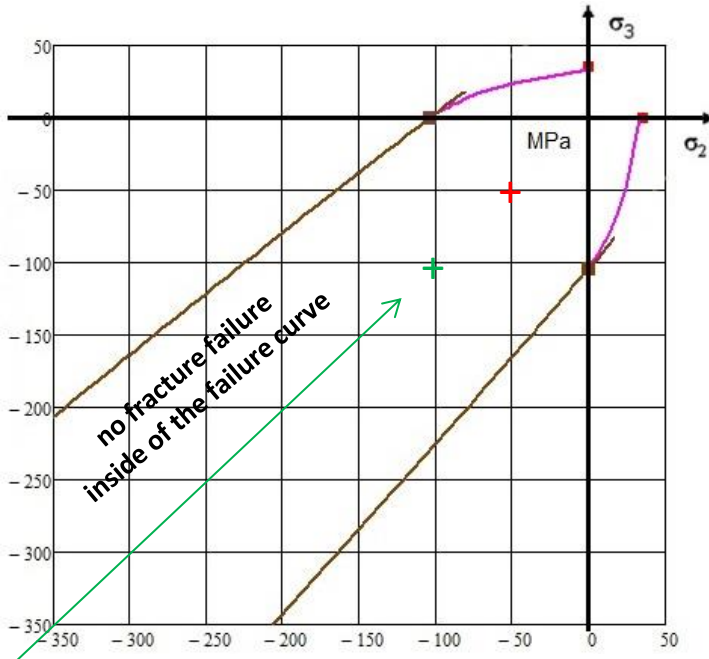

3 stress states and its Eff values

Stress States			Eff in %
	σ_2	σ_3	
1D	0	$-R_\perp^c$	100
2D	$-0.5\ R_\perp^c$	$-R_\perp^c$	24 +
σ^{cc}, σ^{cc}	$-R_\perp^c$	$-R_\perp^c$	**-52** +
			$a_{\perp\perp} = 0.26,\ b_{\perp\perp} = a_{\perp\perp} + 1$
			proportional stressing

Achtung:
Es steigt keine Festigkeit sondern die Schubbruchgefahr Eff wird kleiner !!

- Multiaxial compression lowers the *Eff* of IFF2.
- In the case of 'dense' UD materials bi-axial compression causes no fracture failure, formally indicated by a **negative *Eff***, which physically means *Eff* = 0.
- bi-axial compression generates a tensile stress because the constraining fibers withstand the axial straining.

Finally the application: **Assessment of a Chosen Stress Data Set in the Loop Groove**

3D Stress state: General, modes FF1, FF2, IFF1, IFF2, IFF3

$$\{\sigma\} = (\sigma_1,\ \sigma_2,\ \sigma_3, \tau_{23},\ \tau_{31},\ \tau_{21})^T = (\sigma_1,\ \sigma_2^{pr}, \sigma_3^{pr},\ 0,\ \tau_{31}^{pr},\ \tau_{21}^{pr})^T = (\sigma_{\parallel},\ \sigma_{\perp 2},\ \sigma_{\perp 3}, \tau_{\perp\perp},\ \tau_{\perp\parallel 3},\ \tau_{\perp\parallel 2})^T$$

$$\left\{\sigma_{eq}^{mod\,e}\right\} = \left(\sigma_{eq}^{\parallel\sigma},\ \sigma_{eq}^{\parallel\tau},\ \sigma_{eq}^{\perp\sigma},\ \sigma_{eq}^{\perp\tau},\ \sigma_{eq}^{\parallel\perp}\right)^T \text{ with } \{\bar{R}\} = (\bar{R}_{\parallel}^t, \bar{R}_{\parallel}^c, \bar{R}_{\perp}^t, \bar{R}_{\perp}^c, \bar{R}_{\perp\parallel})^T \quad \text{when mapping}$$

Acting 3D Stress state, caused by 'bias' load situation: i*nner layer*, *higher tan gential stress*

stress dedications: $\sigma_x = \sigma_1 = \sigma_{\parallel}$ (see VDI figure, slide 10),

$\sigma_y = \sigma_{radial} = \sigma_{\perp 3}$ (from zero to compressive maximum in the groove, where $\sigma_{\parallel}$ is also highest).

$\{\sigma\} = (\sigma_1,\ \sigma_2,\ \sigma_3, \tau_{23},\ \tau_{31},\ \tau_{21}) = (1700, -80, -100,\ 10,\ 20,\ 40)$ *in MPa*. *Chosen*

a full 3D assessment is required in Design Verification and not i.e. two 2D-plane assessments, only

Other Input: Strength Design Allowables, curve parameters etc. *Chosen example*, *in MPa*

$$\{\bar{R}\} = (2560,\ 1590,\ 73,\ 185,\ 90)^T \rightarrow \{R\} = (R_{\parallel}^t, R_{\parallel}^c, R_{\perp}^t, R_{\perp}^c, R_{\perp\parallel})^T = (2000,\ 1300,\ 50,\ 140,\ 60)^T$$

$$\mu_{\perp\parallel} = 0.21,\ \mu_{\perp\perp} = 0.206,\ a_{\perp\perp} = \mu_{\perp\perp} / (1 - \mu_{\perp\perp}) = 0.26,\ \nu_{\perp\parallel} = 0.32,\ m = 2.6,$$

$$\{E\} = (165000,\ 165000,\ 8400,\ 8400,\ 5600)^T \text{ MPa}.$$

$$Eff^m = (Eff^{\parallel\sigma})^m + (Eff^{\parallel\tau})^m + (Eff^{\perp\sigma})^m + (Eff^{\perp\tau})^m + (Eff^{\perp\parallel})^m \rightarrow Eff = \left(()^m + ()^m + ()^m + ()^m + ()^m\right)^{m^{-1}}$$

$$Eff_{IFF} = \left((Eff^{\perp\sigma})^m + (Eff^{\perp\tau})^m + (Eff^{\perp\parallel})^m\right)^{m^{-1}}.$$

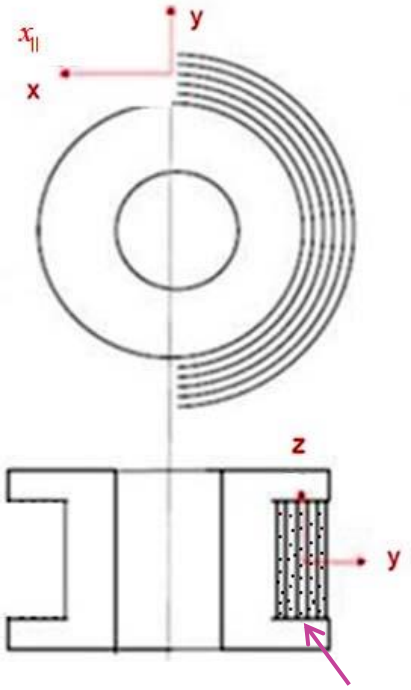

caused by side walls of the groove:

$$\varepsilon_{\parallel} = -\nu_{\perp\parallel} \cdot (\sigma_2^c + \sigma_3^c) / E_{\parallel}$$
$$= -\nu_{\parallel\perp} \cdot (\sigma_2^c + \sigma_3^c) / E_{\perp}.$$
$$\sigma_{1,bi-axial} = E_{\parallel} \cdot \varepsilon_{\parallel}.$$

Results without compressive constraining by stiff side 'walls': Interaction heavily acts, similar to stability !

$Eff^{\parallel\sigma} = 0.74,\ Eff^{\parallel\tau} = 0,\ Eff^{\perp\sigma} = 0,\ Eff^{\perp\tau} = 0.94,\ Eff^{\perp\parallel} = 0.30,\ Eff^{IFF} = 0.95,\ Eff = 1.12$

Results with compressive constraining by stiff side 'walls': Mandatory design !

$Eff^{\parallel\sigma} = 0.75,\ Eff^{\parallel\tau} = 0,\ Eff^{\perp\sigma} = 0,\ Eff^{\perp\tau} = 0.08,\ Eff^{\perp\parallel} = 0.30,\ Eff^{IFF} = 0.31,\ Eff = 0.78.$

Interesting Information on 3D compressive stress states: *Ultra-High-Performance-Concrete UHPC [IfM Dresden]*

Impact of hydrostatic compression on strength capacity.

1D- and 3D-test results → *Eff* remains 100% for $(-\bar{R}^c = -160,\ 0,\ 0)$ and $(-224 - 6,\ -6,\ -6)$.

Lessons Learned: *Eff* = 100% : The (technical) strength is not increased. *Eff* is 100% for both the two failure states

Conclusions

regarding the 3D-stress state in the ‘groove’ of the thimble

1. A SFC has to map 3D stress states. It can be validated, principally, by 3D-test data sets only. If just 2D test data is available, then the necessary 3D mapping quality is not fully proven.
2. Each failure stress state belongs to *Eff* = 100% and represents one point on the surface of the failure body. This is valid for 1D- (these are the strength values), for 2D- and for 3D-stress states
3. In the case of a multiaxial compressive stress state the strength does not increase but the risk to fracture may become smaller, indicated by *Eff* which becomes lower than *Eff* ($R_{\perp}^{c}$ = 100 % !
4. No ‘usual side walls’: A 1D-compressive radial stress state in the groove of the thimble would lead to IFF2-caused wedge failure of the laterally compression-loaded UD loop strand
5. With side walls: The radial compression generates a positively acting 3D-compressive stress state. Hence, side walls of the groove are mandatory despite of the fact that the fibers experience a little higher tensile stress.
6. Hooked fibers or tapes practically do not carry the desired tensile loading. Fibers or tapes loosing some stretch, caused by the winding or tape-laying process, carry much less tensile loading and are not efficiently used.
7. Thin tapes (layers) help to exploit the capacity of the fibers.
8. Reducing the bond between the layers increases the strength capacity of the loop *[CarboLink idea]*.

→ ***Design ‘makes’ structural Strength,*** **q.e.d.**

→ Material symmetry seems to have told the author – after 30 years of (re-)search- :

In the case of transversely-isotropic materials for the associated quantities a generic (basic) number of 5 is inherent.

This is valid for fracture modes, invariants, yield strengths, fracture strengths, and more.

This valuable experience enabled to make an adequate 3D-stress assessment in the turning location.

MIND:

The so-called failure index $|F|$ does not generally give an accurate measure for a stress state if $Eff < 100\%$.

It only fits for the real 'Onset-of-failure' state, where $Eff = 100\% = 1$ and $F = 1$. $Eff < 100\%$:

Usually, the Failure Index $|F|$ is not corresponding to *Eff (see additional slide)*

Standard question and FAQ: What about the porosity in the Strand??

Cuntze's **Novel** Model to map the influence of porosity on the strength capacity of the bi-axially compressed UD-Strand

---

* Failure Function for a dense UD material

$$F^{SF} = [a_{\perp\perp} \cdot I_2 + b_{\perp\perp} \cdot \sqrt{I_4}] \; / \; \bar{R}_{\perp}^{c} = 1$$

$$= [a_{\perp\perp} \cdot (\sigma_2 + \sigma_3) + b_{\perp\perp} \cdot \sqrt{(\sigma_2 - \sigma_3)^2 + 4\tau_{23}{}^2}] \; / \; \bar{R}_{\perp}^{c} = 1$$

with $a_{\perp\perp} = b_{\perp\perp} - 1$ after inserting $\bar{R}_{\perp}{}^{c} = 104$ MPa

* Failure Function for a porous UD material (index po, *author's simple approach*)

$$F^{SF}_{porosity} = \sqrt{a_{\perp\perp po}{}^2 \cdot I_2{}^2 + b_{\perp\perp po}{}^2 \cdot I_4} - a_{\perp\perp po} \cdot I_2 \;] \; / \; 2\bar{R}_{\perp}^{c} = 1$$

$$= \sqrt{a_{\perp\perp po}{}^2 \cdot (\sigma_2 + \sigma_3)^2 + b_{\perp\perp po}{}^2 \cdot \sigma_2 - \sigma_3)^2 + 4\tau_{23}{}^2} - a_{\perp\perp po} \cdot (\sigma_2 + \sigma_3) \;] \; / \; 2\bar{R}_{\perp}^{c} = 1$$

The two curve parameters are determined here from insertion of the compressive strength point $(\sigma_2 = -\bar{R}_{\perp}^{c},\ 0)$ and bi-axial compressive fracture stress point $(\sigma_2 = -\bar{R}_{\perp}^{cc},\ \sigma_3 = -\bar{R}_{\perp}^{cc})$.

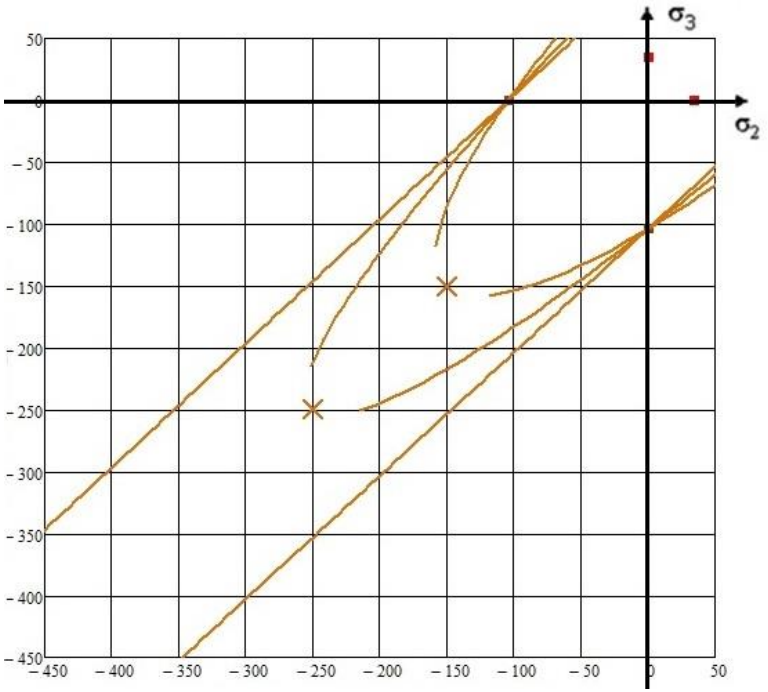

Fracture failure curves of UD material regarding two different porosity grades.

$a_{\perp\perp po}$ for 0, 0.10, 0.22 with $b_{\perp\perp po}$ for 4.0, 3.5, 2.9 .

- Ideal dense materials possess no porosity.
- A fully porous material may be defined by $R_{\perp}{}^{cc} \cong R_{\perp}{}^{c}$.
  This case can be modelled like foam materials in the quasi-isotropic domain [*Cun16a*].

NOTIONS

Condition versus criterion: $F = 1$ versus $F <=> 1$

Damage (Beschädigung): physical harm, which captures in English as well micro-damage (Schädigung) as macro-damage (Schaden)

Eff: material stressing effort *Eff* = f (*Eff* ^{modes}) representing as interaction equation - *captures the damaging portions of all activated modes* - the mathematical equation of the surface of the fracture (failure) body

Equivalent stress σ_{eq}: (a) equivalent to the stress state, as performed in σ_{eq}^{Mises}, and (b) comparable to the value of the strength *R* which dominates one single failure mode or failure type. *Eff* , equivalent stress and strength *R* are positive-defined.

Failure: state of inability of an item to perform a required function in its limit state. A structural part does not fulfil its functional requirements such as the failure modes Onset-of-Yielding, brittle fracture (NF, SF, Crushing Fracture CrF), Fiber-Failure FF, Inter-Fiber-Failure IFF (matrix failure), leakage, deformation limit (tube widening), delamination size limit, frequency bound, or heat flow etc. A failure is a project-defined 'defect'. For each failure mode a Limit State with *F* = Limit State Function or Failure Function is to formulate.

Failure Mode: Failure mode is a commonly used generic term for the types of failures, is a name for a potential way a system may fail (in design verification usually a project- associated failure)

Failure Surface and Failure Body: the surface of the failure body is the shape defined by *F* = 1 or *Eff* = 100% = 1

Failure Type (isotropic): NF, SF, CrF, Normal Yielding NY, Shear Yielding SY

Flaw versus micro-crack: a micro-crack is a sharp flaw (Ungänze), grade of singularity is decisive

Fracture: separation of a whole into parts

Fracture (failure) body: Surface of the tips of all fracture (failure stress) vectors. Fracture is the failure of brittle materials

Material: 'homogenized' (macro-)model of the envisaged complex solid or heterogeneous material combination which principally may be a metal, a lamina or further a laminate stack analyzed with effective properties. Homogenizing (smearing) simplifies modelling

Material behavior: *brittle* behavior could be characterized with the complete loss of tensile strength capacity at first fracture, R^t. Quasi-brittle behavior shows - after reaching R^t - a slight strain hardening followed by a gradual decay of tensile strength capacity during a strain softening domain. *Ductile* behavior is accompanied by a gradual increase of tensile stress (strain hardening), and after reaching R^t a strain softening domain follows

Material Stressing Effort (*Werkstoffanstrengung, nicht Werkstoffausnutzung, das Verschnitt etc berücksichtigt*): definition as $Eff = \sigma_{eq} / R$; max*Eff* =100% is reached at *F* = 1 = 100%. Just for 100% *F* corresponds to *Eff*

'Modal' versus 'Global' SFCs: Modal means that only a test data set of one failure mode domain is mapped whereas global (Drucker-Prager isotropic, Tsai UD) means that mapping is performed over several mode domains. The bottle-neck of global SFCs respectively 'Single Failure Surface Descriptions ' is, that any change in one of the 'forcibly married' modes requires a new global mapping which changes the failure curve in the physically not met mode, too. The advantage of 'Modal' SFCs is to obtain – analogously to Mises - physically plausible equivalent stresses for each failure mode

Multi-fold stress state: example isotropic material: $\sigma_I = \sigma_{II}$, $\sigma_I = \sigma_{II} = \sigma_{III} \rightarrow \sigma_{hyd}$; 3-fold)

Proportional loading: procedure, how the material stressing effort *Eff* is derived from the failure function *F*. In the case of a non-homogeneous function *F* the associated values are only equal for the failure state *F* = 1, respectively for *Eff* = 100%

Reserve factor: ratio of a 'resistance value' and a so-called 'action value'. *RF* > 1 permits a further increase of loading. This is terminated by *Eff* = 100% 'material stressing effort' (Werkstoffanstrengung) in the last critical Hot Spot, when no more stress redistribution in the structural component is possible

Strength: in engineering linked to a uni-axial fracture stress. (1) Characteristic strength: in mechanical engineering the typical average strength, in civil engineering a reduced (5% fractile) average strength value. (2) Design strength: a statistically reduced average strengt. $\overline{R}$ = bar over the *R* which means *average* strength and which is to apply when mapping, like here. *R* = general strength and also the statistically reduced 'strength design allowable.

Stress (not stress component!): component of the stress tensor defined as force divided by the area of cross-section.

Validation: result of a successful qualification of a model (i.e. material model)

(design) Verification: fulfillment of a set of design requirement data

[Cun97] Cuntze R G, Deska R, Szelinski B, Jeltsch-Fricker R, Meckbach S, Huybrechts D, Kopp J, Kroll L, Gollwitzer S, and Rackwitz R: *Neue Bruchkriterien und Festigkeitsnachweise für unidirektio-nalen Faserkunststoffverbund unter mehrachsiger Beanspruchung –Modellbildung und Experimente–*. VDI-Fortschrittbericht, Reihe 5, Nr. 506 (1997), 250 pages. (*New fracture criteria (Puck's criteria) and Strength 'Proof of Design' for Uni-directional FRPs subjected to Multi-axial States of Stress –Model development and experiments*-. In German)

[Cun04] Cuntze R: *The Predictive Capability of Failure Mode Concept-based Strength Criteria for Multidirectional Laminates*. WWFE-I, Part B, Comp. Science and Technology 64 (2004), 487-516

[Cun05] Cuntze R.: *Is a costly Re-design really justified if slightly negative margins are encountered? Konstruktion*, März 2005, 77-82 and April 2005, 93-98 (reliability treatment of the problem)*

[Cun12] Cuntze R: *The predictive capability of Failure Mode Concept-based Strength Conditions for Laminates composed of UD Laminas under Static Tri-axial Stress States*. - Part A of the WWFE-II. Journal of Composite Materials 46 (2012), 2563-2594

[Cun12] HSB 02000-01 *Essential topics in the determination of a reliable reserve factor*. TIB Hannover, 20 pages

[Cun13] Cuntze R: *Comparison between Experimental and Theoretical Results using Cuntze"s „Failure Mode Concept" model for Composites under Triaxial Loadings* - Part B of the WWFE-II. Journal of Composite Materials, Vol.47 (2013), 893-924

[Cun14] Cuntze R: *The Fracture Failure Surface of Foams, derived on basis of the author's Failure Mode Concept*. PPT presentation, Carbon Composites e.V. (CCeV), meeting of the working group 'Engineering', July 11, 2014*

[Cun 14b] Cuntze R: The WWFEs I and II for UD Materials – valuable attempts to validate failure theories on basis of more or less applicable test data. In Conference Handbook SSMET 2014:= Europ. Conf. on Spacecraft Structures, Materials and Environmental Testing. Braunschweig, 1- 4 April 2014, 8 pages

[Cun15a] Cuntze, R.: Static & Fatigue Failure of UD-Ply-laminated Parts – a personal view and more. ESI Group, Composites Expert Seminar, Uni-Stuttgart, January 27-28, keynote presentation*

[Cun16a] Cuntze R: Fracture failure surface of the foam Rohacell 71G. 3. NAFEMS Regionalkonferenz, 25.-27. April, 2016. Berechnung und Simulation, 35 slides*

[Cun16b] Cuntze R: Introduction to the Workshop - from Design Dimensioning via Design Verification to Product Certification. Experience Composites 16 (EC16), September 21 – 23, 2016, Augsburg. Extended Abstract in the Symposium Abstracts. 10 pages*

[Cun16c] Cuntze R: *Progress reached, in Static Design and Lifetime Estimation*? Mechanik-Kolloquium, TU-Darmstadt, December 21, 2016 (UD and isotropic materials, Extended Presentation, 150 slides)*

[Cun17] Cuntze R: *Fracture Failure Bodies of Porous Concrete Stone (foam-like), Normal Concrete, Ultra-High-Performance-Concrete and of the Lamella (sheet) - generated on basis of Cuntze's Failure-Mode-Concept (FMC).* NWC 2017, June 11-14 Stockholm. Extended Abstract, Symposium Handbook, 13 pages

[Cun19a] Cuntze R: presentation in his CU AG "Engineering" on *3D-Festigkeitsbedingungen für spröde Werkstoffe isotrop, transversal–isotrope UD-Schicht und orthotropes Gewebe - ermittelt auf Basis des Failure-Mode-Concepts (FMC) von Cuntze*. June 25, 2019 Basel*

[Cun19c] Cuntze R: Technical terms for composite components in civil engineering and mechanical engineering. Fachbegriffe mit Erklärung und Definition. In: *Fachbegriffe für Kompositbauteile – Technical terms for composite parts*. Springer Vieweg, Wiesbaden, 2019, 171 pages . See*

[Cun20b] Cuntze R: *Normal Yielding NY and Compression-induced Critical Stress Intensity Factor* $K_{IIcr}{}^{c}$ *- Missing Links in an Isotropic 'Closed' Macro-Mechanics Building*. 30 pages*

*https://www.carbon-connected.de/Group/CCeV.Fachinformationen/Dokumente/Documents/Index/10381

Is an accurate Assessment of Stress States by failure index |*F*| and *Eff* given??

We try to calculate the stresses as accurate as possible, but we don't take care enough about strength assessment.
0 < Eff < 100% : For instance the Failure Index |F| does very often not correspond to Eff.
I hope that my reasoning below will lead to a fruitful discussion in future.

SFCs may be mathematically homogeneous or in-homogeneous.
Therefore, the stress assessment measures used must be checked how reliable they are.
Used measures are the **absolute value of the failure function |*F*|** (see Tsai !) delivering a so-called failure index |*F*| and the material reserve factor f_{Res}, an adequate and physically reasonable measure, which is related to the so-called **material stressing effort** $\boldsymbol{Eff^{mode}}$ (Werkstoffanstrengung) by $f_{Res} = 1 / Eff$.

Homogeneous mathematical function *F*

* Concept of proportional loading (stressing):

$$F^{IFF1} = [I_2 + \sqrt{I_4}] / 2\bar{R}_\perp^c = [(\sigma_2{}^p + \sigma_3{}^p) + \sqrt{(\sigma_2{}^p - \sigma_3{}^p)^2 + 0^2}] / 2\bar{R}_\perp^c \quad : \text{no difference between } |F| \text{ and } Eff$$

$$\rightarrow [(\sigma_2{}^p + \sigma_3{}^p) + \sqrt{(\sigma_2{}^p - \sigma_3{}^p)^2}] / (2\bar{R}_\perp^c \cdot Eff^{\perp\sigma}) = 1 \quad \Rightarrow \quad Eff^{\perp\sigma} \equiv [(\sigma_2{}^p + \sigma_3{}^p) + \sqrt{(\sigma_2{}^p - \sigma_3{}^p)^2}] / 2\bar{R}_\perp^c$$

$$F^{IFF2} = [a_{\perp\perp} \cdot I_2 + b_{\perp\perp} \cdot \sqrt{I_4}] / \bar{R}_\perp^c = [a_{\perp\perp} \cdot (\sigma_2{}^p + \sigma_3{}^p) + b_{\perp\perp} \cdot \sqrt{(\sigma_2{}^p - \sigma_3{}^p)^2}] / \bar{R}_\perp^c \quad : \text{no difference between } |F| \text{ and } Eff$$

$$\rightarrow [a_{\perp\perp} \cdot (\sigma_2{}^p + \sigma_3{}^p) + b_{\perp\perp} \cdot \sqrt{(\sigma_2{}^p - \sigma_3{}^p)^2}] / (\bar{R}_\perp^c \cdot Eff^{\perp\tau}) \quad \Rightarrow \quad Eff^{\perp\tau} \equiv a_{\perp\perp} \cdot (\sigma_2{}^p + \sigma_3{}^p) + b_{\perp\perp} \cdot \sqrt{(\sigma_2{}^p - \sigma_3{}^p)^2}] / \bar{R}_\perp^c$$

$$F^{IFF3,\ 2D} = \tau_{21} / (\bar{R}_{21} - \mu_{\perp\parallel} \cdot \sigma_2) \quad \text{..... Linear Mohr-Coulomb}$$

$$\frac{\tau_{21}}{Eff^{IFF3,\ 2D}} / (\bar{R}_{21} - \mu_{\perp\parallel} \cdot \frac{\sigma_2}{Eff^{SF}_{Mohr}}) = 1 \rightarrow Eff^{IFF3,\ 2D} = \frac{\tau_{21} + \mu_{\perp\parallel} \cdot \sigma_2}{\bar{R}_{21}} \quad \text{not permitted}$$

* Concept of factorizing the driving stress. Driving stress = 0 $\rightarrow$ $Eff = 0$, *physically reasonable* : difference between $|F|$ and Eff

$$\frac{\tau_{21}}{Eff^{IFF3,\ 2D}} / (\bar{R}_{21} - \mu_{\perp\parallel} \cdot \sigma_2) = 1 \quad \rightarrow \quad Eff^{IFF3,\ 2D} = \frac{\tau_{21}}{\bar{R}_{21} - \mu_{\perp\parallel} \cdot \sigma_2} \quad \text{permitted}$$

Non-homogeneous mathematical function *F*

: difference between $|F|$ and Eff

* Concept of proportional loading (stressing):

$$F = [a \cdot I_2 + b \cdot I_4 / \bar{R}_\perp^c] / \bar{R}_\perp^c = [a \cdot (\sigma_2 + \sigma_3) + b \cdot (\sigma_2 - \sigma_3)^2 / \bar{R}_\perp^c] / \bar{R}_\perp^c$$

$$\rightarrow [a \cdot (\sigma_2 + \sigma_3) / Eff + b \cdot (\sigma_2 - \sigma_3)^2 / (\bar{R}_\perp^c \cdot Eff^2)] / (\bar{R}_\perp^c) = 1 \quad \Rightarrow \quad Eff \equiv \frac{a \cdot (\sigma_2 + \sigma_3) \pm \sqrt{a^2 \cdot (\sigma_2 + \sigma_3)^2 + 4b \cdot (\sigma_2 - \sigma_3)^2 \cdot \bar{R}_\perp^c}}{2 \cdot \bar{R}_\perp^c}.$$

Linking the Friction Parameter $a_{\perp\perp}$ to the friction value $\mu_{\perp\perp}$

$$\begin{Bmatrix}\varepsilon_1\\ \varepsilon_2\\ \varepsilon_3\\ \gamma_{23}\\ \gamma_{13}\\ \gamma_{12}\end{Bmatrix} = \begin{bmatrix} \frac{1}{E_{||}} & \frac{-\nu_{||\perp}}{E_\perp} & \frac{-\nu_{||\perp}}{E_\perp} & 0 & 0 & 0 \\ \frac{-\nu_{\perp||}}{E_{||}} & \frac{1}{E_\perp} & \frac{-\nu_{\perp\perp}}{E_\perp} & 0 & 0 & 0 \\ \frac{-\nu_{\perp||}}{E_{||}} & \frac{-\nu_{\perp\perp}}{E_\perp} & \frac{1}{E_\perp} & 0 & 0 & 0 \\ & & & \frac{1}{G_{\perp\perp}} & 0 & 0 \\ & (symm.) & & & \frac{1}{G_{||\perp}} & 0 \\ & & & & & \frac{1}{G_{||\perp}} \end{bmatrix} \cdot \begin{Bmatrix}\sigma_1\\ \sigma_2\\ \sigma_3\\ \tau_{23}\\ \tau_{13}\\ \tau_{12}\end{Bmatrix}$$

$Eff^{\perp\tau} \equiv F^{IFF2} = [a_{\perp\perp}\cdot I_2 + b_{\perp\perp}\cdot\sqrt{I_4}] \,/\, \bar{R}_\perp^c = 1, \quad a_{\perp\perp} = b_{\perp\perp} - 1$ after inserting $\bar{R}_\perp^c$

$= [a_{\perp\perp}\cdot(\sigma_2+\sigma_3) + b_{\perp\perp}\cdot\sqrt{(\sigma_2-\sigma_3)^2+4\tau_{23}^2}] \,/\, \bar{R}_\perp^c = 1$

$= [a_{\perp\perp}\cdot(\sigma_2{}^p+\sigma_3{}^p) + b_{\perp\perp}\cdot\sqrt{(\sigma_2{}^p-\sigma_3{}^p)^2+0^2}] \,/\, \bar{R}_\perp^c = 1$ ← 2 structural stresses

$= [a_{\perp\perp}\cdot(\sigma_n+\sigma_t) + b_{\perp\perp}\cdot\sqrt{(\sigma_n-\sigma_t)^2+4\tau_{nt}^2}] \,/\, \bar{R}_\perp^c = 1$ ← 3 Mohr stresses.

* Derivation of the IFF2 slope equation in Mohr stresses: $\sigma_\lambda = 0$

$$\frac{dF}{d\sigma_n}\cdot\bar{R}_\perp^c = a_{\perp\perp} + b_{\perp\perp}(\sigma_n-\sigma_t)/\sqrt{(\sigma_n-\sigma_t)^2+4\tau_{nt}^2}, \quad \frac{dF}{d\tau_{nt}}\cdot\bar{R}_\perp^c = 4\cdot b_{\perp\perp}\tau_{nt}/\sqrt{(\sigma_n-\sigma_t)^2+4\tau_{nt}^2}$$

$$\frac{d\tau_{nt}}{d\sigma_n} = -\frac{dF}{d\sigma_n}/\frac{dF}{d\tau_{nt}} = -\left[\frac{b_{\perp\perp}\cdot(\sigma_n-\sigma_t) + (b_{\perp\perp}-1)\cdot\sqrt{(\sigma_n-\sigma_t)^2+4\tau_{nt}^2}}{4\cdot b_{\perp\perp}\cdot\tau_{nt}}\right], \text{ impl. differentiation}$$

* Transformed structural stresses and addition theorems used: $\tau_{23} = 0$

$$\sigma_n = c^2\cdot\sigma_2 + s^2\cdot\sigma_3, \ \sigma_t = s^2\cdot\sigma_2 + c^2\cdot\sigma_3, \ \tau_{nt} = -s\cdot c\cdot\sigma_2 + s\cdot c\cdot\sigma_3;$$

$s^2+c^2=1, \ S^2+C^2=1, \ C = c^2-s^2 = 2c^2-1, \ S = 2sc, \ c^2 = (C+1)\cdot 0.5, \ s^2 = (1-C)\cdot 0.5$

$\sigma_n+\sigma_t = \sigma_2+\sigma_3, \ \sigma_n-\sigma_t = C\cdot(\sigma_2-\sigma_3), \ \tau_{nt} = -s\cdot c\cdot(\sigma_2-\sigma_3) = -0.5\cdot S\cdot(\sigma_2-\sigma_3)$

* Derivation of transformation relations for equalizing the angle in the touch point

$$\frac{d\tau_{nt}}{d\Theta_{fp}} = \frac{d(-s\cdot c\cdot\sigma_2 + s\cdot c\cdot\sigma_3)}{d\Theta_{fp}} = (s^2-c^2)\cdot(\sigma_2-\sigma_3), \quad \frac{d\sigma_n}{d\Theta_{fp}} = -2\cdot s\cdot c\cdot(\sigma_2-\sigma_3)$$

$$\frac{d\tau_{nt}}{d\sigma_n} = \frac{(s^2-c^2)\cdot(\sigma_2-\sigma_3)}{-2\cdot s\cdot c\cdot(\sigma_2-\sigma_3)} = \frac{C}{S}, \text{ valid if } \textit{uni}\text{- and if } \textit{bi}\text{-}\textit{axial} \text{ (like isotropic)}$$

In the touch point the curve must have the same slope:

$$\frac{d\tau_{nt}}{d\sigma_n} = \frac{C}{S} \leftrightarrow \frac{d\tau_{nt}}{d\sigma_n} = -\left[\frac{b_{\perp\perp}\cdot(\sigma_n-\sigma_t) + (b_{\perp\perp}-1)\cdot\sqrt{(\sigma_n-\sigma_t)^2+4\tau_{nt}^2}}{4\cdot b_{\perp\perp}\cdot\tau_{nt}}\right]$$

After inserting $\sigma_n-\sigma_t = C\cdot(\sigma_2-\sigma_3) = C\cdot\eta$ vanishes σ_t

$$\frac{C}{S} = -\left[\frac{b_{\perp\perp}\cdot(C\cdot\eta) + (b_{\perp\perp}-1)\cdot\sqrt{(C\cdot\eta)^2+4\cdot(-0.5\cdot S\cdot\eta)^2}}{4\cdot b_{\perp\perp}\cdot(-0.5\cdot S\cdot\eta)}\right]$$

Dividing by S and η delivers the fracture angle measure C that defines $b_{\perp\perp} = a_{\perp\perp}+1$

$$C = -\left[\frac{b_{\perp\perp}\cdot C + (b_{\perp\perp}-1)\cdot\sqrt{C^2+4\cdot(-0.5\cdot(1-C^2))^2}}{4\cdot b_{\perp\perp}\cdot(-0.5)}\right] \Rightarrow C = C_{fp}{}^c = -1+\frac{1}{b_{\perp\perp}}.$$

* Mohr, linear fracture condition: $\tau_{nt} = R^\tau - \mu_{\perp\perp}\cdot\sigma_n$ *or* $F = \frac{\tau_{nt}}{R^\tau-\mu\cdot\sigma_n} = 1$

$$\frac{d\tau_{nt}}{d\sigma_n} = -\frac{dF}{d\sigma_n}/\frac{dF}{d\tau_{nt}} = -\frac{\tau_{nt}\cdot\mu}{(R^\tau-\mu\cdot\sigma_n)^2}/\frac{1}{R^\tau-\mu\cdot\sigma_n} = -\frac{\tau_{nt}\cdot\mu}{(R^\tau-\mu\cdot\sigma_n)} = -\mu \equiv \frac{C_{fp}{}^c}{S_{fp}{}^c}$$

* Relations between all friction-linked parameters including $a_{\perp\perp}$ as friction parameter

$\mu_{\perp\perp} = -\tan\rho = -C_{fp}{}^c / S_{fp}{}^c$, for small angles $\cong -C_{fp}{}^c$, further $\tan\phi \equiv \tan\rho$

$b_{\perp\perp} = \frac{1}{C_{fp}{}^c+1} \cong \frac{1}{1-\mu}$ and if an angle is measured $\rightarrow C_{fp}{}^c = \cos\left(\frac{2\cdot\Theta_{fp}^c{}^\circ}{180^\circ}\cdot\pi\right)$.

$\Rightarrow C_{fp}^c = -0.174, \ \Theta_{fp}{}^\circ = 51^\circ, \ a_{\perp\perp} = 0.26, \ \mu_{\perp\perp} = 0.18 \cong -C_{fp}^c.$

IFF3: $F_{\perp\parallel} = \frac{I_3^2}{\bar{R}_{\perp\parallel}^{\,4}} + b_{\perp\parallel} \cdot \frac{I_2 \cdot I_3 - I_5}{\bar{R}_{\perp\parallel}^{\,3}} = 1$

with $I_2 = \sigma_2 + \sigma_3$, $I_3 = \tau_{21}^2 + \tau_{31}^2$, $I_5 = (\sigma_2 - \sigma_3) \cdot (\tau_{31}^2 - \tau_{21}^2) - 4 \cdot \tau_{23}\tau_{31}\tau_{21}$, $I_{23-5} = 2 \cdot \sigma_2 \cdot \tau_{21}^2 + 2 \cdot \sigma_3 \cdot \tau_{31}^2 + 4 \cdot \tau_{23}\tau_{31}\tau_{21}$

The transfer of the SFC to a Mohr-shaped one is directly possible because the fracture plane is already known to be parallel to the fibre direction via $(\tau_{n1},\ \sigma_n) \equiv (\tau_{21},\ \sigma_2)$, $|\tau_{21}| = \bar{R}_{\perp\parallel} - \mu_{\perp\parallel} \cdot \sigma_2$

FMC: $\frac{\tau_{21}^4}{\bar{R}_{\perp\parallel}^{\,4}} + b_{\perp\parallel} \cdot \frac{2 \cdot \sigma_2 \cdot \tau_{21}^2}{\bar{R}_{\perp\parallel}^{\,3}} = 1 \rightarrow \frac{\tau_{nt}^2}{\bar{R}_{\perp\parallel}^{\,4}} + b_{\perp\parallel} \cdot \frac{2 \cdot \sigma_n \cdot \tau_{nt}^2}{\bar{R}_{\perp\parallel}^{\,3}} = 1 \rightarrow \sigma_n = \frac{\bar{R}_{\perp\parallel}^{\,3} \cdot \left(\frac{\tau_{21}^4}{\bar{R}_{\perp\parallel}^{\,4}} - 1 \right)}{2 \cdot \tau_{nt}^2 \cdot b_{\perp\parallel}}$ and Mohr: $\tau_{nt1} = \bar{R}_{\perp\parallel} - \mu_{\perp\parallel} \cdot \sigma_n \rightarrow \sigma_n = \frac{\bar{R}_{\perp\parallel} - \tau_{nt1}}{\mu_{\perp\parallel}}$

$\frac{d\tau_{nt}}{d\sigma_n} \rightarrow$ simpler to perform is FMC : $\frac{d\sigma_n}{d\tau_{nt}} = \frac{2 \cdot \tau_{nt}}{\bar{R}_{\perp\parallel} \cdot b_{\perp\parallel}} - \frac{\bar{R}_{\perp\parallel}^{\,3} \cdot \left(\frac{\tau_{nt}^4}{\bar{R}_{\perp\parallel}^{\,4}} - 1 \right)}{\tau_{nt}^3 \cdot b_{\perp\parallel}}$ and Mohr : $\frac{d\sigma_n}{d\tau_{nt}} = \frac{-1}{\mu_{\perp\parallel}}$

In the strength point equal slope and $\tau_{n1} = \bar{R}_{\perp\parallel}$

$\frac{2 \cdot \tau_{nt}}{\bar{R}_{\perp\parallel} \cdot b_{\perp\parallel}} - \frac{\bar{R}_{\perp\parallel}^{\,3} \cdot \left(\frac{\tau_{21}^4}{\bar{R}_{\perp\parallel}^{\,4}} - 1 \right)}{\tau_{nt}^3 \cdot b_{\perp\parallel}} = \frac{-1}{\mu_{\perp\parallel}} \rightarrow b_{\perp\parallel} = \frac{\mu_{\perp\parallel} \cdot \left(\bar{R}_{\perp\parallel}^{\,4} + \tau_{nt}^4 \right)}{\tau_{nt}^3 \cdot b_{\perp\parallel}} \Rightarrow b_{\perp\parallel} = 2 \cdot \mu_{\perp\parallel}$. A good guess for μ is sufficient for application.

3D or 3D-reduced use of general SFC-formula:

$\frac{I_3^2}{\bar{R}_{\perp\parallel}^{\,4}} + b_{\perp\parallel} \cdot \frac{I_2 \cdot I_3 - I_5}{\bar{R}_{\perp\parallel}^{\,3}} = 1$ or $\frac{\tau_{21}^4}{\bar{R}_{\perp\parallel}^{\,4}} + b_{\perp\parallel} \cdot \frac{2 \cdot \sigma_2 \cdot \tau_{21}^2}{\bar{R}_{\perp\parallel}^{\,3}} = 1$ always with $b_{\perp\parallel} = 2 \cdot \mu_{\perp\parallel}$

or in Eff

$Eff^{\perp\parallel} = \{[2\mu_{\perp\parallel} \cdot I_{23-5} + (\sqrt{(2\mu_{\perp\parallel})^2 \cdot I_{23-5}{}^2 + 4 \cdot \bar{R}_{\perp\parallel}{}^2 \cdot (\tau_{31}^2 + \tau_{21}^2)^2}\,]/(2 \cdot \bar{R}_{\perp\parallel}{}^3)\}^{0.5}$; 2D SFC: $\{[b_{\perp\parallel} \cdot 2\sigma_2 \cdot \tau_{21}{}^2 + \sqrt{(b_{\perp\parallel} \cdot 2\sigma_2 \cdot \tau_{21}{}^2)^2 + 4\bar{R}_{\perp\parallel}{}^2 \cdot \tau_{21}{}^4}\,]/2\bar{R}_{\perp\parallel}$

2*D* use of simple SFC-formula (= Mohr): $\mu \cong (\tau_{21,fr} - \bar{R}_{\perp\parallel}) / \sigma_{2,fr}$

$|\tau_{21}| = \bar{R}_{\perp\parallel} - \mu_{\perp\parallel} \cdot \sigma_2$ with $\mu_{\perp\parallel}$ measured or determined from curve fitting or less complicated from two curve points.

All Results: $\Rightarrow$ $\mu_{\perp\perp} = -\cos(2 \cdot \theta_{fp}^{c}\,^{\circ} \cdot \pi / 180^{\circ})$, $b_{\perp\perp} \cong 1 / (1 - \mu_{\perp\perp})$, $b_{\perp\parallel} \cong 2 \cdot \mu_{\perp\parallel}$ with $0.05 < \mu_{\perp\parallel} < 0.3$, $0.05 < \mu_{\perp\perp} < 0.2$,

UD-material: UD cube, Material Properties and 2D-interaction equation

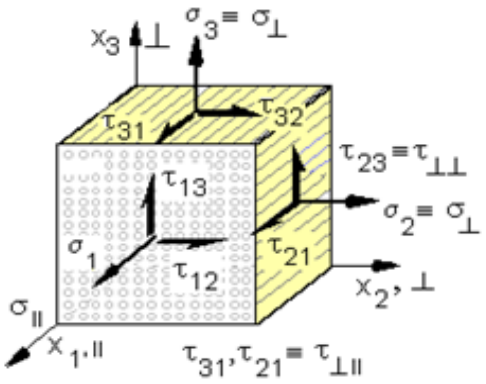

$$\{\sigma\}=(\sigma_1,\sigma_2,\sigma_3,\tau_{23},\tau_{13},\tau_{12})^T$$

$$R_{\parallel}^{t},\ R_{\parallel}^{c},\ R_{\perp\parallel},\ R_{\perp}^{t},\ R_{\perp}^{c}$$

$$E_{\parallel},\ E_{\perp},\ G_{\parallel\perp},\ \nu_{\perp\parallel},\ \nu_{\perp\perp}$$

$$R_{\parallel}^{t}(=X^t),\ R_{\parallel}^{c}(=X^c),\ R_{\perp\parallel}(=S),\ R_{\perp}^{t}(=Y^t),\ R_{\perp}^{c}(=Y^c)$$

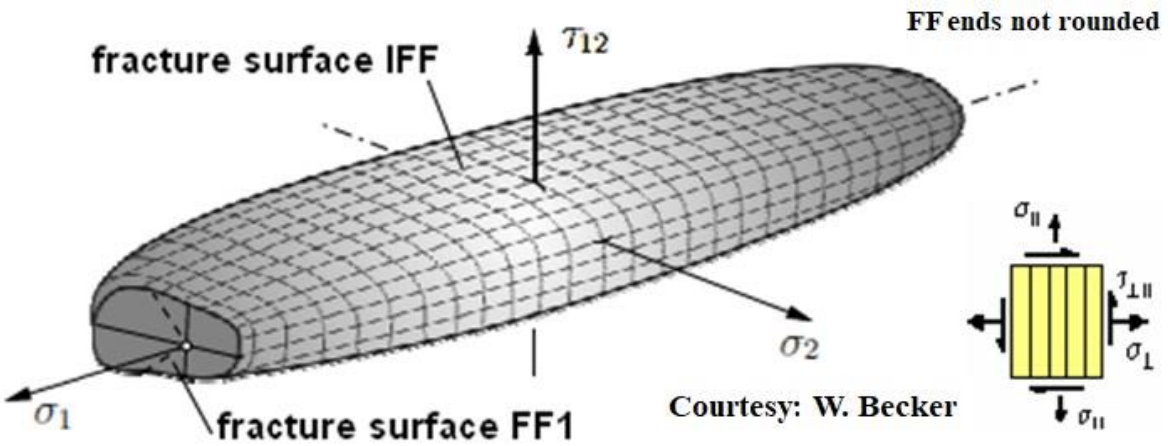

$$\left[\frac{\varepsilon_1^t\cdot E_{\parallel}}{R_{\parallel}^t}\right]^m+\left[\frac{-\varepsilon_1^c\cdot E_{\parallel}}{R_{\parallel}^c}\right]+\left(\frac{\sigma_2}{R_{\perp}^t}\right)^m+\left(\frac{|\tau_{21}|}{R_{\perp\parallel}-b_{\perp\parallel}\cdot\sigma_2)}\right)^m+\left(\frac{-\sigma_2}{R_{\perp}^c}\right)^m=1$$

$$b_{\perp\perp}=1/(1-\mu_{\perp\perp})$$

LL: Unfortunately, the US-designations were chosen non-self explaining which also confuses in continuum mechanics. And even worse: These letters found entrance into the FEA-manuals !

UD Material: Visualisation of Fracture Body and formulation of '2-fold' Fracture Body

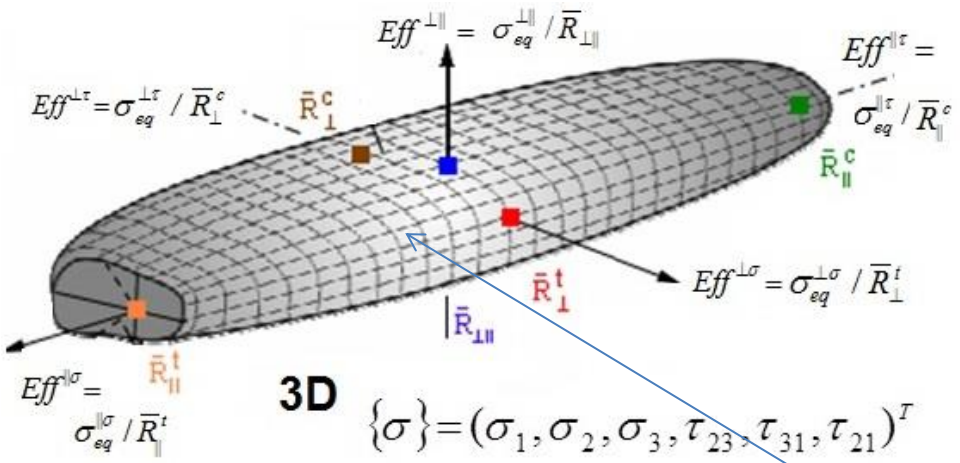

$$\left\{\sigma_{eq}^{mode}\right\} = \left(\sigma_{eq}^{\parallel\sigma},\ \sigma_{eq}^{\parallel\tau},\ \sigma_{eq}^{\perp\sigma},\ \sigma_{eq}^{\perp\tau},\ \sigma_{eq}^{\parallel\perp}\right)^T$$

For the **2D (plane) stress state** the visualization of the associated fracture (onset) body is still possible in fracture stresses. *In this context, mind that in general 2D stress states nevertheless may activate all 5 modes!*

$$Eff^m = (Eff^{\parallel\tau})^m + (Eff^{\parallel\sigma})^m + (Eff^{\perp\sigma})^m + (Eff^{\perp\tau})^m + (Eff^{\perp\parallel})^m$$

For the **3D stress state** a fracture body of stresses cannot be drawn due to too much stresses, namely 6 and 5 at least after transformation into the quasi-isotropic plane.

The τ may be further combined, because these possess a common action plane but without a successful reduction. Also the use of the 5 invariants does not help compared with the simple isotropic case with 2 (I_1, J_2) or 3 (J_3) invariants.

However, moving from stresses to the equivalent stresses σ_{eq} or the associated Effs delivers the desired 3D-body.

The left figure shows that the visualization of the 3D fracture stress state id s possible by applying *Effs*.

The interaction equation should capture the multi-fold acting of a failure mode:

$$Eff^m = (Eff_{\parallel}^{\tau})^m + (Eff_{\parallel}^{\sigma})^m + (Eff_{\perp}^{\sigma})^m + Eff_{\perp}^{MfFd} + (Eff_{\perp}^{\tau})^m + (Eff_{\perp\parallel})^m = 1$$

considering $\sigma_2^t = \sigma_3^t$ and $\sigma_2^c = \sigma_3^c$

and $Eff_{\perp}^{MfFd} = (\sigma_2^t + \sigma_3^t) / 2\bar{R}_{\perp}^{tt}$, with $\bar{R}_{\perp}^{tt} \approx \bar{R}_{\perp}^{t} / \sqrt[m]{2}$ [Awaji]

with $\bar{R}_{\perp}^{tt} \le \bar{R}_{\perp}^{t}$, $\bar{R}_{\perp}^{cc} \ge \bar{R}_{\perp}^{c}$ if dense and not porous

LL:
Puck uses Mohr stresses in his IFF interaction approach. Puck's angle-dependent stress exposure f_E cannot fully correspond to Cuntze's effort Eff_{IFF} (IFF1, IFF2 +IIFF) because f_E belongs to his Mohr-based, combined IFF-approach. This requires the determination of the fracture plane angle Θ_{fp}. If $Eff^{\perp\parallel} \gg Eff^{\perp\tau}$ then $\Theta_{fp} = 0$, max $\Theta_{fp} = \Theta_{fp}^{c}$.

UD-material Information

UD material is a transversely-isotropic material. Inherent, due to material symmetry reasons, are generic numbers for material quantities: 5 strengths, 5 elasticity quantities and 2 for the so-called physical properties

Loading (civil engineering terms):

ULS Ultimate Limit State, SLS Servicability Limit State

Structural stresses, principal stresses and equivalent stresses:

$\{\sigma\} = (\sigma_1,\ \sigma_2,\ \sigma_3, \tau_{23},\ \tau_{31},\ \tau_{21})^T$, $\{\sigma\}^{pr} = (\sigma_1,\ \sigma_2^{pr}, \sigma_3^{pr},\ 0,\ \tau_{31}^{pr},\ \tau_{21}^{pr})^T$

$\left\{\sigma_{eq}^{\mathrm{mod}\,e}\right\} = \left(\sigma_{eq}^{\|\sigma},\ \sigma_{eq}^{\|\tau},\ \sigma_{eq}^{\perp\sigma},\ \sigma_{eq}^{\perp\tau},\ \sigma_{eq}^{\|\perp}\right)^T$

Strengths (Resistances):

$\{\bar{R}\} = (\bar{R}_{\|}^{t}, \bar{R}_{\|}^{c}, \bar{R}_{\perp}^{t}, \bar{R}_{\perp}^{c}, \bar{R}_{\perp\|})^T$ average, mean, typical, characteristic values for Test Data Analysis

(in civil engineering: characteristic means slightly reduced average value, 5% quantile)

$\{R\} = (R_{\|}^{t}, R_{\|}^{c}, R_{\perp}^{t}, R_{\perp}^{c}, R_{\perp\|})^T$ statistically reduced average value for Design Verification

Physical properties:

$(E_{\|} = E_1,\ E_{\perp} = E_2 = E_3,\ G_{\|\perp} = G_{12},\ \nu_{\perp\perp} = \nu_{23},\ \nu_{\perp\|} = \nu_{21})$

average values to be used to obtain the best realistic result = a 50% expected value.

For Design Verification - according to the project task - minimum or maximum values are to apply

Stress - strain curve is a physical property. It must be applied as average curve in order to obtain the most realistic deformation of the structure and of the to be determined cross-section quantities for the design.

Only in rare statically-determined applications it might be applied to directly capture design verification.

Unfortunately, this is often violated in civil engineering codes and in mechanical engineering as well.

Friction values to be provided for analysis in case of compression are $(\mu_{\perp\perp},\ \mu_{\perp\|})$.

Coefficients of Thermal Expansion $(\alpha_{T\|},\ \alpha_{T\perp})$, *Coefficient of Moisture Expansion* $(\alpha_{M\|},\ \alpha_{M\perp})$

Pre-design Input for Cuntze's 3D UD SFCs (strength criteria)

	Test Data Mapping	Design Verification
	$\{\bar{R}\} = (\bar{R}^t_{\|\|}, \bar{R}^c_{\|\|}, \bar{R}^t_{\perp}, \bar{R}^c_{\perp}, \bar{R}_{\perp\|\|})^T$,	$\{R\} = (R^t_{\|\|}, R^c_{\|\|}, R^t_{\perp}, R^c_{\perp}, R_{\perp\|\|})^T$
• **5 strengths :**	average (typical) values	strength design allowables

- **2 friction values :** for 2D $\mu_{\|\perp}$, for 3D $\mu_{\|\|}$, $\mu_{\perp\perp}$
- **Poisson's ratios :** for 2D $\nu_{\|\|}$, for 3D $\nu_{\|\|}$, $\nu_{\perp\perp}$
- **1 mode-interaction exponent :** m for 2D and 3D
- **Values, recommended for pre-design**: $\nu_{\|\|}$ = 0.3, $\nu_{\perp\perp}$ = 0.35, $\mu_{\|\|}$ = 0.1, $\mu_{\perp\perp}$ = 0.1, m = 2.6
- **No more input required than for the usually applied, global strength failure conditions** such as Tsai-Wu **! No fiber properties necessary.**

A good estimation for CFRP and GFRP (the error in the range of ± 5 % is smaller than the test scatter) reduces the number of five independent elastic properties to four.

$$\nu_{\perp\perp} \approx \nu_{\perp\|}(1-\nu_{\perp\|} \cdot E_{\perp} / E_{\|}) / (1-\nu_{\perp\|})$$

LL:

- From experience and due to the usually too few test data sets and the scatter → for all interaction zones the same interaction exponent value m is chosen, *for practical engineering reasons !*
- The less symmetry restrictions are the more independent elastic properties a material possesses.

UD Material: Numerically Robust 3D and 2D (fracture) Failure Mode Interaction

When automatically inserting the FEA stress output into all 5 equations some Eff^{modes} may become negative which mechanically means zero. As still indicated before: This is by-passed by using the formulations.

2D failure condition & failure surface :

$$\left(\frac{(\varepsilon_1+|\varepsilon_1|)}{2\bar{R}^t_{||}}\cdot E_{||}\right)^m + \left(\frac{-\varepsilon_1+|\varepsilon_1|}{2\bar{R}^c_{||}}\cdot E_{||}\right)^m + \left(\frac{\sigma_2+|\sigma_2|}{2\bar{R}^t_{\perp}}\right)^m + \left(\frac{|\tau_{21}|}{\bar{R}_{\perp||}-\mu_{\perp||}\cdot\sigma_2}\right)^m + \left(\frac{-\sigma_2+|\sigma_2|}{2\bar{R}^c_{\perp}}\right)^m = 1$$

3D failure condition & failure surface:

$$\left(\frac{(\varepsilon_1+|\varepsilon_1|)}{2\bar{R}^t_{||}}\cdot E_{||}\right)^m + \left(\frac{-\varepsilon_1+|\varepsilon_1|}{2\bar{R}^c_{||}}\cdot E_{||}\right)^m + \left(\frac{(I_2+\sqrt{I_4})+|I_2+\sqrt{I_4}|}{4\bar{R}^t_{\perp}}\right)^m +$$

$$+\left(\frac{-[(\mu_{\perp\perp}-1)I_2+\mu_{\perp\perp}\sqrt{I_4}]+|[(\mu_{\perp\perp}-1)I_2+\mu_{\perp\perp}\sqrt{I_4}]|}{2\bar{R}^c_{\perp}}\right)^m +$$

$$+\sqrt{\frac{2\mu_{\perp||}\cdot I_{23-5}+\left(\sqrt{(2\mu_{\perp||})^2\cdot {I_{23-5}}^2+4\cdot {\bar{R}_{\perp||}}^2\cdot(\tau_{31}^2+\tau_{21}^2)^2}\right)}{2{\bar{R}_{\perp||}}^3}} = 1$$

Enabling an Automatic Use of the Failure Conditions in 3D Applications

$$I_2=\sigma_2+\sigma_3\ ,\quad I_3=\tau_{31}^2+\tau_{21}^2,\quad I_4=(\sigma_2-\sigma_3)^2+4\tau_{23}^2,$$

$$I_{23-5}=2\sigma_2\cdot\tau_{21}^2+2\sigma_3\cdot\tau_{31}^2+4\tau_{23}\tau_{31}\tau_{21}$$

$$\left\{Eff^{mode}\right\}=\begin{Bmatrix}0, & Eff^{mode}<0\\ Eff^{mode}, & Eff^{mode}\geq 0\end{Bmatrix}$$

- **The vector of the modes' equivalent stresses reads**

$$\left\{\sigma_{eq}^{mode}\right\}=\left(\sigma_{eq}^{||\sigma},\ \sigma_{eq}^{||\tau},\ \sigma_{eq}^{\perp\sigma},\ \sigma_{eq}^{\perp\tau},\ \sigma_{eq}^{||\perp}\right)^T \qquad 2.5\leq m\leq 3$$

LL:
- An equivalent stress is always positive such as the strength.
- It includes all actual load stresses and the residual stresses (from curing etc.) that are acting together in a given mode.

Basics-reminder of the Hashin-Puck UD Action Plane Conditions for Onset of IFF

Paul's modification of the Mohr-Coulomb Hypothesis [Pau??]: " Brittle (behaving) material will fracture in either that plane where the shear stress τ_{nt} reaches a critical value which is given by the shear resistance of a fiber-parallel plane increased by a certain amount of friction caused by the simultaneously acting compressive stress σ_n on that plane. Or, it will fracture in that plane, where the maximum principal (tensile) stress reaches the transverse tensile strength $R_{\perp}^{t}$ (is in the quasi-isotropic plane)"

Hashin Hypothesis, stated in [Has80] 1980: "From some (traditional, global) criteria follows, that failure under biaxial tensile stresses depends on the values of the compressive failure stress. This is physically unacceptable! The foregoing difficulties provide the motivation to re-present the failure criterion of a UD fibre composite in *piece-wise smooth* form, where each branch represents one distinct failure mode." And further, "It should be emphasized that the choice of quadratics is based on curve fitting and not on physical reasoning! The quadratic is the simplest presentation, which can fit the data reasonably well. It is unfortunate that the quadratic nature of stress-energy-density forms has at times led to a physical interpretation of quadratic failure criteria or of quadratic initial yielding criteria in plasticity". "The failure criterion has to be - due to transversal isotropy - invariant under any rotation around the fibre axis. Therefore, the criterion can be at most a function of the UD stress invariants I_1, I_2, I_3, I_4 under such a rotation. "In the event that a failure plane - under an angle Θ_{fp} - can be identified, the failure is produced by the normal and shear stresses on that plane". On this argument he created the following failure criterion for ***tension***, in which the unknown angle Θ_{fp} of the always fibre parallel fracture planes has to be inserted :

$\sigma_n > 0$: IFF is caused by the combination of $\sigma_n^{\,t}$, τ_{nt} , τ_{n1} $\quad \Rightarrow \quad F_{IFF} = \left(\frac{\sigma_n(\Theta_{fp})}{\bar{R}_{\perp}^{\,t}} \right)^2 + \left(\frac{\tau_{nt}(\Theta_{fp})}{\bar{R}_{\perp\perp}} \right)^2 + \left(\frac{\tau_{n1}(\Theta_{fp})}{\bar{R}_{\perp\parallel}} \right)^2 = 1$

Hashin termed $R_{\perp\perp}$ that strength which causes fracture under pure transversal shear. As we have to deal with brittle materials $R_{\perp\perp}$ simply corresponds to $R_{\perp}^{t}$. The tensile stress component (the other stress component is compressive) of the shear stress drives this NF. "A different failure criterion should be used for ***compression*** $\sigma_n < 0$. Failure will occur on the plane defined by a Θ_{fp} which makes the left side of the compressive failure criterion a maximum. Failure would then be given – as before - for $\Theta = \Theta_{fp}$. The procedure is somewhat reminiscent of Mohr's failure theory as used in soil mechanics etc. While it may appear attractive because of its sound physical basis, it is unfortunately difficult to use". He proposed a modified Mohr-Coulomb IFF approach but did not pursue this idea due to numerical difficulties (at that time).

Also in this paper Hashin included an invariant-based global quadratic interpolation approach which combines the IFFs ('matrix modes'). However the author did not grasp all of the UD invariants he used, ending with 2 of the 3 IFFs. The failure surface of these invariant-based SFCs is not continuous. In view of his *choice of a quadratic approximation (now he does it like the others he criticized above)* he excluded I_5 , which captures the physical difference between $\tau_{21}(\sigma_2)$ and $\tau_{21}(\sigma_3)$.

Puck: As early as 1969 Puck proposed conditions for fibre failure (FF, 2 separate FF modes) and for inter-fibre failure (IFF, consisting of the 3 IFF modes). In 1991 he elaborated Hashin's IFF hypothesis. *He bases his IFF conditions on Mohr-Coulomb and Hashin and interacts the 3 Mohr stresses $\sigma_n, \tau_{nt}, \tau_{n1}$ on the IFF fracture plane. He uses simple polynomials (parabolic or elliptic)to formulate a so-called master fracture body in the $\sigma_n, \tau_{nt}, \tau_{n1}$ space.* He used inclination parameters p (representing friction analogous to Cuntze's $b_{\perp\perp}$, $b_{\perp\parallel}$), which are determined from fracture curves for different stress combinations. Puck's model was simplified by specifying only one inclination parameter, p, which has certain stability advantages, see the work by R. Jeltsch-Fricker, presented in [Cun97 et. al.] showing a simplified parabolic IFF model. In order to capture the common failure danger or interaction between his 2 FF SFCs and the combined IFF SFC he proposed a weakening factor that takes care of the reduced IFF strength due to premature breakage of single fibres and mode interaction. He discriminates matrices with high or low fracture strain, [VDI 2014].

Cuntze: The author uses 2 FF and 3 invariant-based IFF SFCs (invariants not from Hashin but Boehler) assuming that in each mode condition one stress is the driving stress σ or τ and each mode is associated to a distinct strength that governs this mode. The invariant I_5 is applied !

History

- Since 1985 common search together with Prof. A. Puck (Uni-Gh Kassel) and Dr. M. Gädke (DLR Braunschweig) for improved fracture criteria of the still widely used, light-weight driving material, the transversely-isotropic UD-lamina.
- 1992 – 1997, Investigation of the Hashin/Puck "Action Plane Strength Criterion" (project leader Cuntze, book: VDI-Fortschrittbericht 1997, Nr.506)
- Since 1993 Cuntze 'in parallel' investigated his "Failure Mode Concept" FMC idea based on specific points: (1) v. Mises (HMH) describes by the criterion just one failure mode, the onset of yielding. As approach an invariant J_2 of the isotropic material has been used. It should be possible to transfer this idea from one mode yielding of ductile materials to the multifold fracture modes of brittle materials. Of course, the invariants to be applied (they reflect the material's symmetry) are different for isotropic, transversally-isotropic and further the orthotropic fabric materials. (3) The same physical (mechanical) behaviour facilitates and demands the same failure (mode) description. Existing links in the mechanical behaviour show up: Fully different structural materials can possess similar material behaviour and may belong to the same class of material symmetry. For instance: a brittle porous concrete in the compression domain can be basically described by the same failure condition like a foam or a very ductile behaving light-weight steel in the high multi-axial tension domain when pores (void nucleation) have been generated in the necking cross section of the tensile bar specimen (another example was foam and porous concrete stone). This has the consequence: The same failure function F can be used for different materials and more information is available for pre-dimensioning and modelling from past experimental results of a similarly behaving material.
- WWFE-I (2003) and –II (2012): The private authors, Cuntze with his FMC-based SFCs and Puck with his "Action Plane Strength Criterion", won WWFE-I. In WWFE-II, Cuntze mapped those Test Cases best which have an accurate test data input.
- 2006, publication of VDI 2014, sheet 3 "Development of Fibre-Reinforced Plastic Components. (Editor R. Cuntze. This guideline Includes the matured "Action Plane Strength Criterion" of A. Puck).

Some specifica of the "Failure Mode Concept"

- Concept for any material like metals, composites, concrete, foam, ceramics, .. and a concept for brittle and ductile behaviour
- Application of invariants-based SFCs for each strength failure mode of ductile and brittle behaving materials
- Separation of mechanistic and probabilistic effects considering mode interaction
- No "global fitting" but "mode fitting" of the course of test data in each pure mode domain
- Fracture mechanics (does not consider 3D-states of stress): Idea to bridge the gap from strength mechanics to crack fracture mechanics in the process zone in front of the crack tip, reduction of number of (mixed-mode model-linked) fracture toughness K_{IC}, K_{IIC}, K_{IIIC} to real inherent material properties K_{IC} in tension, K_{IIC} in compression. Primarily, only "stable" fracture planes and Ks should be considered. Might be also in facture mechanics the possibility to interact the fracture modes?
- Similar procedure for transversally-isotropic material (5 fracture toughnesses)
- Continuous transition from yield criteria to fracture criteria *[ESDU data sheet citation: not possible]*
- Successful application to several isotropic and transversely-isotropic materials (2D, 3D)
- Successful transfer to predict constant fatigue life curves. FMC considers the complete state of stress, searches the "critical damaging plane", where the damaging portions, both, from shear and/or normal stress have accumulated worst.

LL:
Transversely-isotropic UD matrials are not so simply homogenizable than isotropic materials. A UD material is internally still 'structured' so that the 'lower level' constituents fiber and matrix determine fracture.

Formulation of the Hashin-Puck FF and IFF Action Plane Conditions

IFF-Hypotheses Mohr, Hashin, Puck, Cuntze:

O. Mohr (isotropic): $F(\sigma_n, \tau_n, R_\sigma, R_\tau, \Theta_{fp}) = 1$

Z. Hashin (UD): $F(\sigma_n, \tau_n, R_\sigma, R_\tau, \Theta_{fp}) = 1$

SFC cannot discriminate $\sigma_2(\tau_{21})$ from $\sigma_3(\tau_{21})$, because invariant I_5 is not used.

A. Puck (UD): $F(\sigma_n, \tau_n, R_\sigma{}^A, R_\tau{}^A, p, \Theta_{fp}) = 1,$

introduced the 'action plane resistances' R^A.

Comparison Cuntze (UD): $F\ (\{\sigma\}, \{R, \mu\}) = 1.$

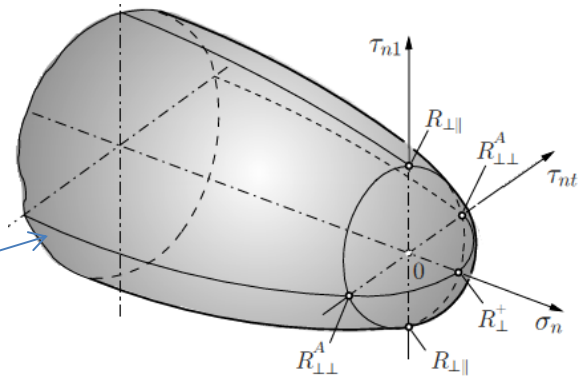

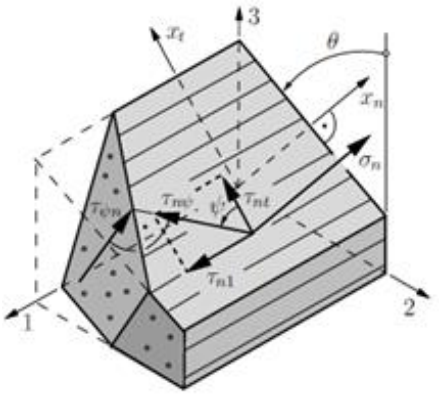

Puck 's FF and combined IFF Strength Conditions:

$\sigma_1 > 0$: $FF1 = \frac{\sigma_1}{\bar{R}^t_\parallel} = 1;$ $\sigma_1 < 0$: $FF2 = \frac{-\sigma_1}{\bar{R}^t_\parallel} = 1;$

$\sigma_n > 0$: IFF is caused by the combination of $\sigma_n{}^t$ and τ_{nt} and τ_{n1} acting in the fracture plane

$$F_{IFF} = \left(\frac{\sigma_n(\Theta_{fp})}{\bar{R}_\perp{}^t}\right)^2 + \left(\frac{\tau_{nt}(\Theta_{fp})}{\bar{R}_{\perp\perp}{}^A}\right)^2 + \left(\frac{\tau_{n1}(\Theta_{fp})}{\bar{R}_{\perp\parallel}}\right)^2 = 1$$

$\sigma_n = 0$ is not a real boundary.

$\sigma_n < 0$: $\sigma_n{}^c$ does not contribute to IFF. It even impedes SF caused by τ_{nt} and τ_{n1} according to an increased material resistance

$$F_{IFF} = \left(\frac{\tau_{nt}(\Theta_{fp})}{\bar{R}_{\perp\perp}{}^A - p_{\perp\perp}\cdot\sigma_n}\right)^2 + \left(\frac{\tau_{n1}(\Theta_{fp})}{\bar{R}_{\perp\parallel} - p_{\perp\parallel}\cdot\sigma_n}\right)^2 = 1$$

with $\Theta \to \Theta_{fp}$ when $F_{IFF}(\Theta) \to \max F_{IFF}$ and p a friction value.

$\bar{R}_{\perp\perp}{}^A = \bar{R}_\perp{}^c / (2 + 2p_{\perp\perp})$.

Considering interaction FF with IFF, see VDI 2014, sheet 3.

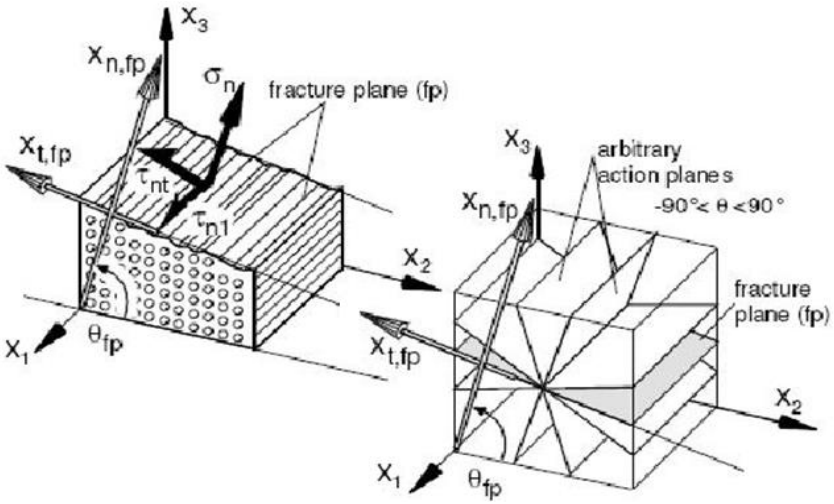

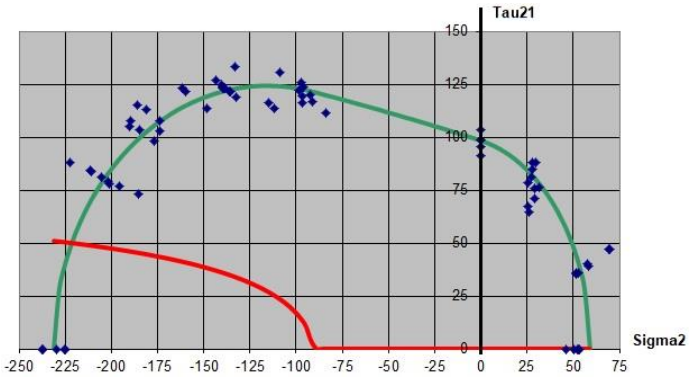

Different to tension, the first term in the compressive equation does not exist, because compressive resistance can be set infinite. Hashin transferred the Mohr hypothesis to UD materials. The red curve at right depicts the increase of Puck's Θ_{fp} with increasing compressive stress.

Shear Curves: Puck and Cuntze

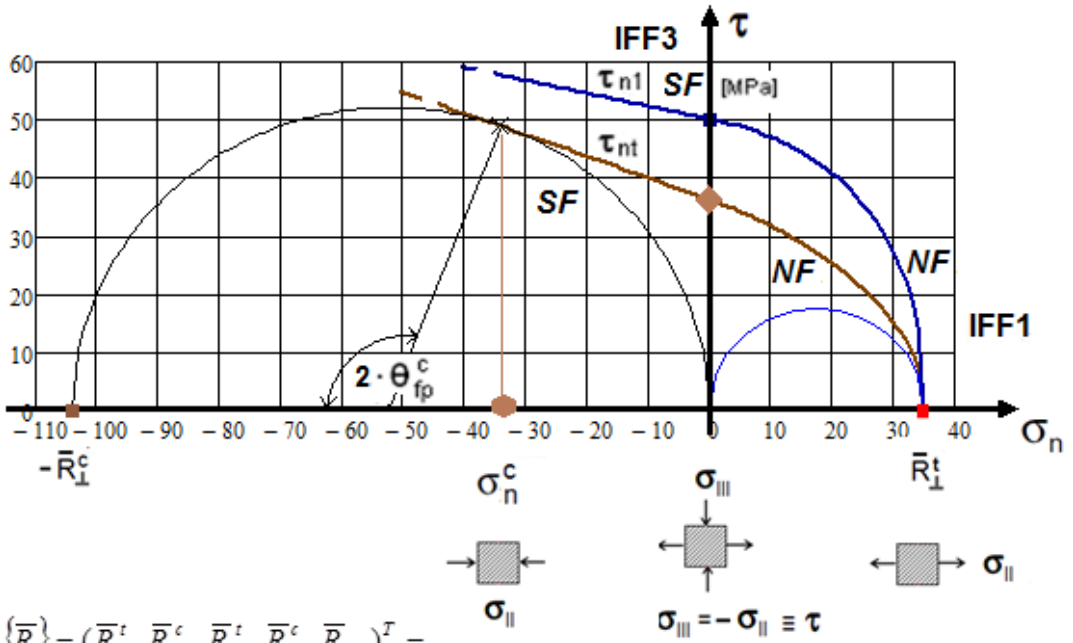

$$\{\bar{R}\} = (\bar{R}_{||}^{t}, \bar{R}_{||}^{c}, \bar{R}_{\perp}^{t}, \bar{R}_{\perp}^{c}, \bar{R}_{\perp||})^{T} =$$

$$(1100, 600, 104, 35, 50)^{T}\ \text{MPa}$$

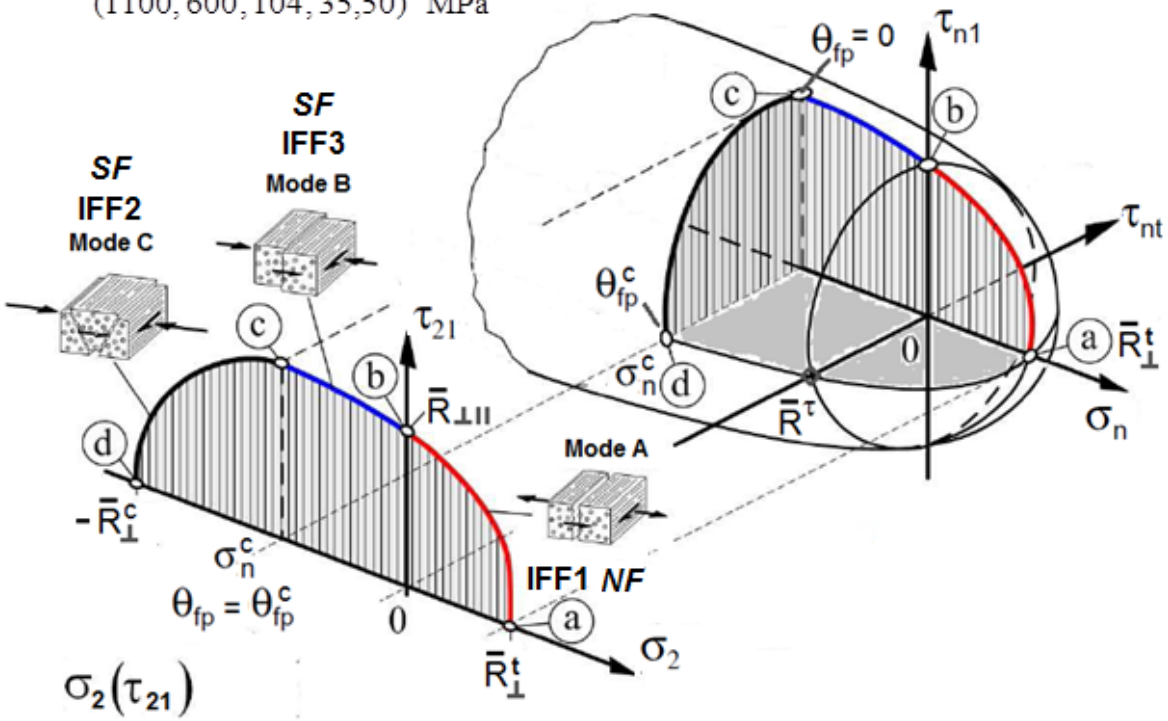

Cuntze's *frature body meridians and angles of fracture (upper figure);* $\mu_{\perp||} = 0.22$, $\mu_{\perp\perp} = 0.36$, $\vartheta_{fp}^{c} = 55°$, $m = 2.5$.

Puck's master (Mohr) fracture body in Mohr coordinates (below) and its main cross sections as well as fracture angles. On the master fracture body the curve parts are colored which are identical to those on the IFF curve.

From $\theta_{fp} = 0$ until θ_{fp}^{c} (around 52°) the Mohr stress σ_n takes the constant value σ_n^{c}.